NON-DESTRUCTIVE CHARACTERIZATION OF PULSE FLOURS FROM DIFFERENT MILLING METHODS

by

Chitra Sivakumar

A Thesis submitted to The Faculty of Graduate Studies of

The University of Manitoba

In partial fulfillment of the requirements for the degree of

MASTER OF SCIENCE

Department of Biosystems Engineering

University of Manitoba

Winnipeg, Canada,

R3T 5V6

THESIS ABSTRACT

With increasing consumer interest in pulse flour-based food formulations, characterization of pulse flours based on pulse-type and milling techniques has become crucial. The present research work is aimed at using non-destructive imaging techniques including visible near-infrared (Vis-NIR) and shortwave infrared (SWIR) hyperspectral imaging and scanning electron microscopy (SEM) for pulse flour characterization. Four different types of pulses namely, chickpea, yellow pea, navy bean, and green lentil milled using a single-stage Ferkar mill and a multistage roller mill were studied. Hyperspectral imaging was used for classifying these flours based on pulse-type and milling methods, through the development of unsupervised and supervised classification models and classification maps. In the case of supervised classification of pulse-type, the wavelength range of 530 to 700 nm contributed to the color attributes of the biological samples yielding 100% classification accuracy. For milling method based supervised classification, the wavelength regions, 1370 to 1500 nm, and 1700 to 2000 nm, that capture the protein content of the flour, yielded 95% classification accuracy. SEM was used to study the microstructural changes of the flours. Stream-based and pulse-type classifications were conducted to study the relationship between particle size distribution and protein content, and characteristics of starch-protein matrices. The findings from SEM images revealed that fine distribution of protein bodies was found in Ferkar milled and straight grade (SG) stream of roller milled flours with similar protein content. On the other hand, the reduction stream had higher protein content and starch damage than the break stream. The presence of pores was higher in chickpea starches for both roller and Ferkar milled flours. Navy bean flours possessed the highest starch-protein cluster count. Traces of bran particles were clearly visible in green lentil flours obtained from roller and Ferkar mills. Hence, from SEM results it can be inferred that the microstructure and protein content of the pulse flours is influenced by the pulse type and milling method. Overall, it can be concluded that non-destructive imaging techniques such as Vis-NIR and SWIR hyperspectral imaging and SEM can prove to be a useful tool for pulse flour characterization based on pulse-type and milling methods.

ACKNOWLEDGEMENT

I am grateful to my advisor, Dr. Jitendra Paliwal, for giving me opportunity to work on the Pulse Cluster Canada project. His constant guidance and support helped me to complete this program successfully. I thank Dr. Rani Ramachandran for her guidance in the beginning of the project as a post doctoral fellow and as a committee member. I thank Dr. Chyngyz Erkinbaev for his invaluable support as a committee member.

I really appreciate Dr. Mudassir Chaudhry and Dr. Mohammad Nadimi, post doctoral fellows for their continuous support during the experiment, data analysis, and thesis writing times. I thank Dr. Catherine Findlay for her support during manuscript writing. I am thankful for the financial assistance through Dr. Paliwal that I received during my research period.

I would like to thank all my friends for their moral support and encouragement during low times.

Finally, I thank my parents and family members.

TABLE OF CONTENTS

LIST OF TABLES

LIST OF FIGURES

MANUSCRIPT SUBMISSIONS

Chapters three and four of this thesis are based on the following submission to peer-reviewed journals.

Chapter 3: **Sivakumar, C.,** M.M.A. Chaudhry., and J. Paliwal. Classification of pulse flours using near-infrared hyperspectral imaging. *(Submitted to LWT)*

Chapter 4: **Sivakumar, C.,** M.M.A. Chaudhry., M. Nadimi, J. Paliwal, and J. Courcelles. Characterization of pulse flours using scanning electron microscopy. *(Submitted to Food and Bioprocess Technology)*

CHAPTER 1. Overview of the thesis

1.1 Scope of the research

Pulses are edible seeds in the family *Fabaceae* that are rich in micro and macro nutrients and form one of the most nutritious parts of human diet. Studies have shown that pulse consumption promotes digestion and weight loss hence lowering the risk of cardio-vascular diseases, diabetes, and cancer (Mudryj et al. 2014). It is noted that plant-based diets are being preferred by health-conscious consumers who have increased awareness of the impact of agricultural practices on the environment (Carlsson-Kanyama and González 2009; Röös et al. 2017). Studies have shown that pulse flour properties and particle size influence the end-quality of food products (Bourré et al.2019; Maskus et al.2016; Young et al.2020). In the modern food industry, adequate knowledge of pulse flour properties is a prerequisite to supply quality products at retail.

Milling method impacts the flour parameters such as starch damage and protein quality which in turn affects the usage of a flour for specific end products. Also, similar looking flours may have different properties as a function of various milling techniques. Blending the flours obtained from different mills changes their overall chemical composition and particle size distribution, which in turn affects the functional and nutritional properties of the flour, affecting the quality of the end products. Employing systematic studies for pulse flour characterization based on pulse type and milling method hold great significance to quality control; however, no standardized characterization of pulse flours exists. To address this need, the present study was conducted to classify pulse flours using near infrared hyperspectral imaging and explore the microstructure of these flours using scanning electron microscopy (SEM).

Hyperspectral imaging is a rapid, reliable, and non-invasive technique for the quality evaluation of food products. The spatial distribution and spectral dimension of the chemical compound can be achieved from hyperspectral imaging as it integrates both imaging and spectroscopic methods (ElMasry and Sun 2010; ElMasry et al. 2012; Su and Sun 2017). Combining spectral information and multivariate data analysis techniques can provide useful insight to characterize food products (Babellahi et al. 2020; Chaudhry et al. 2018). Studies have shown that these techniques have

successfully predicted the chemical composition such as protein, moisture, and starch content in green lentils (Kaliramesh et al. 2013), and isoflavones content in soybeans (Kezhu et al. 2014).

On the other hand, understanding the microstructure of flours can assist in interpreting the transport phenomena. Physical properties such as color, bulk and particle density, and porosity are affected by the transport phenomenon, which in due course influences the physicochemical, functional, and nutritional properties of the flour (Aguilera 2004). The microstructure of flour also affects the bioavailability of the nutrients (Parada and Aguilera 2007). To attain a profound understanding of particle size and component separation, it is essential to explore flour's starch-protein matrix. The scanning electron microscope, with magnification levels of 20 to 10,000 ×, is ideally suited to study starch-protein matrices of flours and could be deployed as a useful tool here (Aguilera and Germain 2007; Assatory et al. 2019; Pelgrom et al. 2013; Schutyser et al. 2015).

1.2 Objectives

The main objective of this research is to classify and explore the microstructure of four different types of pulse flours namely chickpea, navy bean, green lentil, and yellow pea, milled using a single-stage Ferkar mill and multi-stage roller mill. This was accomplished by pursuing the following individual objectives:

- To utilize hyperspectral images in the Vis-NIR (400-1000 nm) and SWIR (1000-2500 nm) regions for the classification of pulse flours based on pulse-type and milling methods.
- To utilize SEM imaging for the assessment of the microstructural changes in flours obtained from two different milling methods, by investigating the particle size distribution and its relationship with protein content; and exploring the starch-protein matrices.

Figure 1.1 shows the experimental design for the research objective.

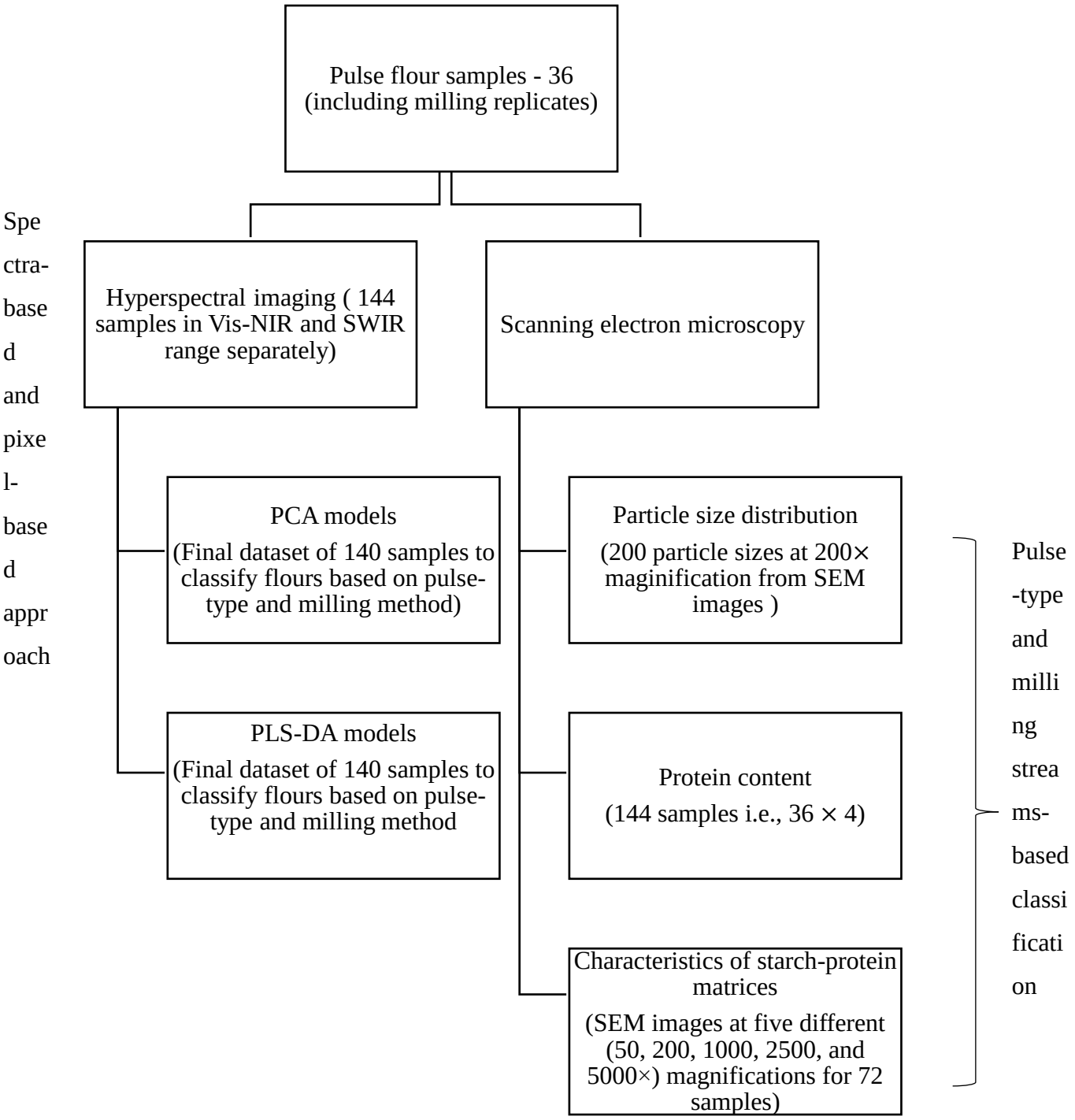

Figure 1.1 Flowchart of the experimental design

1.3 Structure of the thesis

This thesis is comprised of five chapters. Chapter one demonstrates an overview of the research work and its objectives. Chapter two provides a comprehensive literature review. Chapters three and four discuss the objectives, experimental designs, and obtained results of the research in a manuscript-based format (submitted manuscripts). Chapter three is titled “Classification of pulse flours using near-infrared hyperspectral imaging” and chapter four as “Pulse flours characterization using scanning electron microscopy”. The thesis summary and overall conclusion are included in chapter five, followed by recommendations for future research in chapter six.

References

Aguilera, J. M., and J. C. Germain. 2007. Advances in image analysis for the study of food microstructure. *Understanding and Controlling the Microstructure of Complex Foods*. 261–287. https://doi.org/10.1533/9781845693671.2.261.

Aguilera, José Miguel. 2005. Why food micro structure? *Journal of Food Engineering* 67(1–2): 3–11. https://doi.org/10.1016/j.jfoodeng.2004.05.050.

Assatory, A., M. Vitelli , A. R. Rajabzadeh and R. L. Legge. 2019. Dry fractionation methods for plant protein, starch and fiber enrichment: A review. *Trends in Food Science and Technology* 86(February):340–351. https://doi.org/10.1016/j.tifs.2019.02.006.

Babellahi, F., J.Paliwal, C. Erkinbaev, M. L.Amodio, M. M. A. Chaudhry, and G. Colelli. (2020). Early detection of chilling injury in green bell peppers by hyperspectral imaging and chemometrics. *Postharvest Biology and Technology* 162(September 2019), 111100. https://doi.org/10.1016/j.postharvbio.2019.111100.

Carlsson-Kanyama, A., and A. D. González. 2009. Potential contributions of food consumption patterns to climate change. *American Journal of Clinical Nutrition* 89(5):1704S-1709S. https://doi.org/10.3945/ajcn.2009.26736AA.

Chaudhry, M. M. A., M. L. Amodio, F. Babellahi, M. L. V. de Chiara, J. M Amigo Rubio, and G. Colelli. 2018. Hyperspectral imaging and multivariate accelerated shelf life testing (MASLT) approach for determining shelf life of rocket leaves. *Journal of Food Engineering* 238(June): 122–133. https://doi.org/10.1016/j.jfoodeng.2018.06.017.

ElMasry, G., M. Kamruzzaman, D. W. Sun, and P. Allen. 2012. Principles and Applications of Hyperspectral Imaging in Quality Evaluation of Agro-Food Products: A Review. *Critical Reviews in Food Science and Nutrition* 52(11):999–1023. https://doi.org/10.1080/10408398.2010.543495.

ElMasry, G., and W.D. Sun. 2010. Principles of Hyperspectral imaging technology. *Hyperspectral Imaging for Food Quality Analysis and Control*, ed. Da-Wen Sun, 3-45.

London, UK: Academic press.

Kaliramesh, S., V. Chelladurai, D. S. Jayas, K. Alagusundaram, N. D. G. White, and P. G. Fields .2013. Detection of infestation by Callosobruchus maculatus in mung bean using near-infrared hyperspectral imaging. *Journal of Stored Products Research* 52:107–111. https://doi.org/10.1016/j.jspr.2012.12.005.

Kezhu, T., C.Yuhua, S.Weixian, and C. Xiaoda. 2014. Detection of isoflavones content in soybean based on hyperspectral imaging technology. *Sensors and Transducers* 169(4):55–60.

Mudryj, N. Adriana, Yu, Nancy, H. M. Aukema. 2014. Nutritional and health benefits of pulses. *Applied Physiology, Nutrition, and Metabolism* 39:1197–1204.

Parada, J., and J. M. Aguilera. 2007. Food microstructure affects the bioavailability of several nutrients. *Journal of Food Science* 72(2). https://doi.org/10.1111/j.1750-3841.2007.00274.x.

Pelgrom, P. J. M., A. M. Vissers, R. M. Boom, and M. A. I. Schutyser. 2013. Dry fractionation for production of functional pea protein concentrates. *Food Research International* 53(1):232–239. https://doi.org/10.1016/j.foodres.2013.05.004.

Röös, E., B. Bajželj, P. Smith, M. Patel, D. Little, and T. Garnett. 2017. Protein futures for Western Europe: potential land use and climate impacts in 2050. *Regional Environmental Change* 17(2):367–377. https://doi.org/10.1007/s10113-016-1013-4.

Schutyser, M. A. I., P. J. M. Pelgrom, A. J. van der Goot, and R. M. Boom. 2015. Dry fractionation for sustainable production of functional legume protein concentrates. *Trends in Food Science and Technology* 45(2):327–335. https://doi.org/10.1016/j.tifs.2015.04.013.

Su, W. H., and D. W. Sun. 2018. Fourier Transform Infrared and Raman and Hyperspectral Imaging Techniques for Quality Determinations of Powdery Foods: A Review. *Comprehensive Reviews in Food Science and Food Safety* 17(1):104–122. https://doi.org/10.1111/1541-4337.12314.

CHAPTER 2. Literature review

2.1 Importance of pulses

Pulses are dried seeds that belong to the family *Fabaceae* or *Leguminosae.* As crucial dietary components, they play an important role in agriculture, environment, food security, and human nutrition. Pulse crops are known to improve soil fertility by converting atmospheric nitrogen into nitrogen compounds with the help of symbiotic bacteria *(Rhizobium and Bradyrhizobium)* (Hossain et al. 2016). Also, they are an inexpensive source of proteins that have antioxidant and anti-carcinogenic properties due to the presence of phytochemicals, tannins, and saponins (Chan et al. 2010). Pulses, rich in fibre and low in glycemic index, help in maintaining blood glucose and insulin levels for diabetic people (Rizkalla et al. 2002). The dietary fibre present in pulses affects calorie intake by increasing chewing time and satiety, thus helping in weight management (McCrory et al. 2010).

2.2 Nutritional value of pulses used in this study

The widely grown pulses in Canada include dry beans, chickpeas, field peas, and lentils. Pulses are a rich source of carbohydrates, protein, fibre, fat, vitamins, and minerals. They can be classified as starch-rich pulses (such as peas, beans, lentils) and oil-rich rich pulses (such as soybean and groundnut). Pulses used in this study are chickpeas (CDC Orion), green lentils (CDC Greenstar), yellow peas (CDC Spectrum), and navy beans (Nautica).

For chickpeas, the starch content varies from 41 to 50 % with the kabuli variety containing more soluble sugars. The protein content of chickpea varies from 17 to 22 % (Hulse 1991) with crude protein ranging from 12.4 to 31.5%. Moreover, chickpea possesses a low glycemic index due to the lower availability of carbohydrates (Atkinson et al. 2008; Johnson et al. 2005). The fat content in chickpea is around 6% with oleic acid, linoleic acid, linolenic acid, palmitic acid, and stearic acid as essential unsaturated fatty acids (Zia-Ul-Haq et al. 2007); they also include important sterols such as β-sitosterol, stigmasterol, and campesterol (Jukanti et al. 2012). Chickpeas are a good source of vitamins such as β-carotene, riboflavin, niacin, and thiamine (Jukanti et al. 2012), and minerals such as potassium, sodium, magnesium, copper, zinc, iron,

and calcium (Rachwa-Rosiak et al. 2015). In addition to these components, the phenolic compounds in chickpeas contain antioxidant, anti-proliferative, and antimutagenic properties.

Green lentils are a rich source of carbohydrates (57 to 61%), protein (22.5 to 26.4%), fibre (6 to 11%) with low-fat content (1.15 to 1.75%), and traces of vitamins and minerals. The large variation in nutritional composition is due to the variety and processing methods utilized for analysis (Mubarak 2005). Consuming cereals with green lentils provides a complete essential amino acid profile as green lentils contain high content of essential amino acids (Dahiya et al. 2015). The highest and lowest amount of fatty acids present in green lentils are linoleic acid and lauric acid, respectively, with moderate amounts of stearic, behenic, oleic, palmitic, myristic, arachidic, linolenic, and capric acid (Abdel-Rahman et al. 2007; Adsule et al.1986). Vitamins such as riboflavin, pantothenic acid, thiamine, niacin, and nicotinic acids are present, with carotenoids in form of xanthophylls and β-carotene. The green coloured varieties (0.9 mg/100g) contain a high quantity of carotenoids than yellow varieties (0.7 mg/100g). A high percentage of these carotenoids are present in the seed coat of green varieties (Harina and Ramirez 1978). Calcium, magnesium, sodium, potassium, iron, copper, zinc, manganese, and phosphorus are among the common minerals found in green lentils. The quantity of calcium in green lentils is four times greater than that in cereals (Dahiya et al. 2015).

Navy beans are a rich source of carbohydrates (40 to 42%), protein (24 to 26%), fat (1.2 to 1.4%), and fiber (32 to 33%) (Gujska et al.1994). The nutritional composition could vary depending on variety and processing method. They are an excellent source of soluble fibers and B-complex vitamins (thiamine and riboflavin). They contain minerals such as potassium, calcium, phosphorus, and iron with low sodium content (Singh et al. 2015). In addition, they also contain traces of amino acids such as lysine, asparagine, glutamine, arginine, histidine, isoleucine, leucine, threonine, and valine (Bellido 2002).

In peas, starch, protein, and total dietary fiber vary from 36.9 to 49%, 21.2 to 32.9%, and 14 to 26%, respectively. Globulins constitute a majority of proteins with the highest amino acid contents as glutamine, aspartic acid, arginine, lysine, cysteine, tryptophan, and methionine, and the lowest content by cysteine, tryptophan, and methionine. The total lipid content in pea ranges from 1.2 to 2.4% with fatty acids such as linoleic, oleic, palmitic, linolenic, stearic, gadoleic,

erucic, and lignoceric acids. Peas are a dietary source of folate and carotenoids such as lutein, β-carotenes, violaxanthin, and zeaxanthin. The trace minerals found in peas are potassium, magnesium, phosphorous, iron, selenium, zinc, molybdenum, manganese, copper, and boron (Dahl et al. 2012).

2.3 Value-added products from pulse flours

The functional, nutritional, and sensory properties of food formulations can be enhanced by the inclusion of pulses, or pulse-based ingredients with cereal products. Sprouted beans are widely consumed as a fresh salad ingredient whereas pulse flours are widely used in soups, confectionaries, curries, porridges, and alcoholic beverages. Miñarro et al. (2012) formulated bread using chickpea flour, pea isolate, carob germ flour, or soya flour to study the characteristics of gluten-free bread. Their results revealed that chickpea bread yielded the softest crumb with the best physico-chemical characteristics and good sensory attributes. On the contrary, Yamsaengsung et al. (2010) reported an increase in crumb firmness, decrease in bread volume in whole wheat and white bread blended with chickpea flour. Kaack and Pedersen (2005) developed a low-calorie chocolate cake using potato pulps and yellow pea hulls.

As an alternative to cereal-based products, cookies have also been developed using pulse flours. Studies reported an increase in protein, resistant starch, and overall acceptability of the cookies developed from chickpea and green lentil flours (Noor Aziah et al. 2012; Pasha et al. 2011). Han et al. (2010) developed gluten-free crackers from flours of green and red lentils, chickpea, yellow pea, pinto bean, and navy bean flours. Researchers have developed nutritious weaning food using green lentils with germinated wheat (Imtiaz 2007) and potato flour (Bazaz et al. 2016).

Extruded products such as noodles, pasta, spaghetti, and puffed snacks can be made from pulse flours. Noodles have been developed from green lentil flour due to its high starch content (Kasemsuwan et al.1998; Tang et al. 2014). Wang et al. (1999) made pasta from yellow pea flour for gluten intolerant people. Similarly, (Osorio-Díaz et al. 2008) developed a pasta from durum and chickpea flour blend, and reported an increase in nutritional properties such as protein, ash, dietary fiber, and lipid content. Nayak et al. (2011) reported that the puffed product formulated

from purple potato and yellow pea flour was rich in antioxidants. Anton et al. (2008) developed tortillas from navy bean flour with a significant reduction in anti-nutritional factors.

2.4 Pulse processing

The common anti-nutritional factors present in pulses are tannins, trypsin, polyphenols, hemagglutinins, phytic acid, proteinase inhibitor, and trypsin inhibitors. Protease inhibitors and lectins can cause toxicity. The interaction between these anti-nutritional factors with other nutrients in seed decreases their bioavailability. Inhibitors such as trypsin inhibitor, chymotrypsin inhibitor, α-amylase inhibitor, phytohemagglutinin restrict the activity of amino acids (Bellido 2002). Polyphenols, phytic acid, and fibers affect the bioavailability of minerals (Jain et al. 2009). The activity of anti-nutritional factors can be reduced by processing methods such as milling, dehulling, roasting, soaking, germination, fermentation, frying, and grinding (Barakoti and Bains 2007; Dahiya et al. 2015). This reduction in anti-nutritional factors may be attributed to the leaching of anti-nutrients in water due to concentration gradient and formation of insoluble complex compounds during high temperature processing that breaks up the phytic acid (Barakoti and Bains 2007). Tortillas formulated from blends of pulses (pinto, black, red and navy beans) and wheat flour reported a significant reduction in anti-nutritional factors with minor variation in antioxidant activity and phenolic content (Anton et al. 2008). Dahiya et al. (2015) reported processing methods such as soaking, germination, and fermentation significantly reduce the anti-nutritional properties of green lentils.

Pulse milling serves three main objectives *viz.*, reduction of particle size; separation of seed component; and induction of mechano-chemical changes. Pre-milling treatments such as soaking, conditioning, micronization, hydro-thermal treatments, and partial germination affect the milling process by changing the quality attributes of flours and their fractions (Scanlon et al. 2018).

2.5 Milling methods

The commonly used milling methods are stone mill, roller mill, knife mill, pin mill, and hammer mill. Owing to the commercial significance and way of operation, roller and Ferkar mills were used as two different milling methods in this study.

A Roller mill is a type of attrition mill that gives four to five fractions of flours using shear and compression force. Roller mills have two types of rolls i.e., break rolls and reduction rolls. Break rolls have a flute surface where the kernel is broken such that bran remains with larger particles and endosperm can be sifted from bran as it contains small particles. Reduction rolls have smooth and frosted surface. Since the reduction rolls operate at lower differentials, they affect water absorption capacity and baking performance by damaging starch granules (Campbell, 2007). Ferkar mill is a single-stage knife mill i.e., it converts whole seed into one fraction of flour. Uniformly granulated high-quality flour is produced using Ferkar mill. Bourré et al. (2019) reported significant difference in bread-baking properties (viscosity, proofing, mixing time, resilience, colour, texture, softness, crumb strength) and nutritional properties (starch content, starch damage, protein, water absorption capacity, oil absorption capacity) in pulse flours obtained from commercial mills and a Ferkar mill due to different particle sizes. They concluded that whole or dehulled pulses affect the particle size. Also, the effect of pre-milling treatments such as micronization, roasting, and pre-germination milled using Ferkar mills improves baking and functional properties of whole yellow pea flour (Frohlich et al. 2019; Young et al. 2019).

2.5.1 Relationship between particle size and nutritional composition

Previous research works have shown that protein content varies with milling methods and the streams (Maskus et al. 2016; Pelgrom et al. 2013; Thakur et al. 2019). Maskus et al. (2016) reported significant differences in particle size, and nutritional composition such as protein, fiber, and starch content of whole and split yellow pea flour milled using stone mill, coarse and fine pin mill, roller mill, and hammer mill. Their study revealed that stone mill has the highest average particle size followed by hammer mill, roller mill and pin mill where coarse pin mill and roller mill yield similar average particle size. Starch damage was the highest in roller mill and similar protein content was observed in stone and hammer mills. Sakhare et al. (2014) reported that protein content varies in roller milled green lentil flours among its streams. Pelgrom et al. (2013) reported that protein bodies should be smaller than other cell components (starch and fiber) to have optimal separation. Very fine milling damages starch and produces similarly sized protein bodies and starch granules, which in turn leads to inefficient detachment. Too coarse milling, in contrast, has aggregates of cell components following inadequate separation. Hence,

it is necessary to study the particle size distribution and its relationship with cell components to have a better understanding of protein and starch rich fractions.

2.6 Non-destructive analysis of pulse flours

From the previous section, it can be established that nutritional composition of flours depends on milling method and the streams of flour generated by a mill. When flours milled from different mills/streams are blended together, there is a change in chemical composition. This change in chemical composition determines physical, functional, nutritional, and microstructural properties of flours. Consequently, these properties affect the overall acceptance of desired end products. Systematic studies can be employed to characterize the pulse flours based on milling method and pulse-type using non-destructive analysis. The non-destructive analysis such as hyperspectral imaging and scanning electron microscopy are used in this study to characterize the pulse flours.

2.6.1 Hyperspectral imaging

Electromagnetic spectrum is a frequency range consisting of a series of electromagnetic radiations such as ultraviolet rays, x-rays, microwaves, radio waves, gamma rays, visible light, and infrared rays with their wavelengths and photon energies. They are separated into low frequency (long wavelength) and high frequency (short wavelength). Spectrum is produced when photons interact with matter and the study of this interaction of light with matter is known as spectroscopy. Sorting of food and agricultural materials based on visual appearance (colour, morphology or texture) is generally carried out in the visible range (400 to 740 nm) of light. Infrared region (900 to 12000 nm) is commonly used for unravelling the constitutional composition of organic materials including agricultural produce. Hyperspectral imaging (HSI) is a technique where spectra of contiguous wavelengths is collected in a spatially distributed manner providing us the knowledge of the distribution of chemical compounds in a sample. Short wave infrared (970 to 3000 nm) hyperspectral imaging has been widely used to determine the moisture content of grains and to identify foreign materials in feed and food (Fernández Pierna et al. 2012; McGoverin et al. 2011). Researchers have detected and quantified peanut powder and walnut powder traces in whole wheat flour using NIRS and HSI (Mishra et al. 2015;

Zhao et al. 2019, 2018). Therefore, these techniques can be used to classify the milled products for raw material characterization.

Hyperspectral imaging (HSI) is a powerful, rapid, accurate, reliable, and non-invasive method to analyse biological samples. It combines both imaging and spectroscopic methods to provide a detailed analysis of nutritional profile and biochemical distributions within samples. Also, it provides information on spectral dimension of the type of chemical compound present in a sample (ElMasry et al. 2012). Interaction of photons with food at molecular level forms the basis of hyperspectral imaging. The physical and chemical information of sample are stored in form of a complex data unit called hypercube. Both qualitative (e.g., disease infection) and quantitative (e.g., protein content) information can be extracted from hypercubes. The hypercubes can be obtained by one of the following ways.

- Area scan (staring imaging method)
- Point scan (whiskbroom method)
- Line scan (push broom method)

In area scanning mode, image acquisition takes place wavelength-by-wavelength within fixed field-of-view. In point scanning mode, spectra are acquired at points by moving the sample. In line-scan or push broom method, progressive construction of hypercube takes place by collecting spectral data for single spatial line. It uses wavelength dispersive system with the help of a transmissive or reflective diffraction grating or prism techniques. The samples can be moved physically, or the beam and detector are moved to the region of interest. In this study, a line scan system was used, the schematic of which is presented in Figure 2.1.

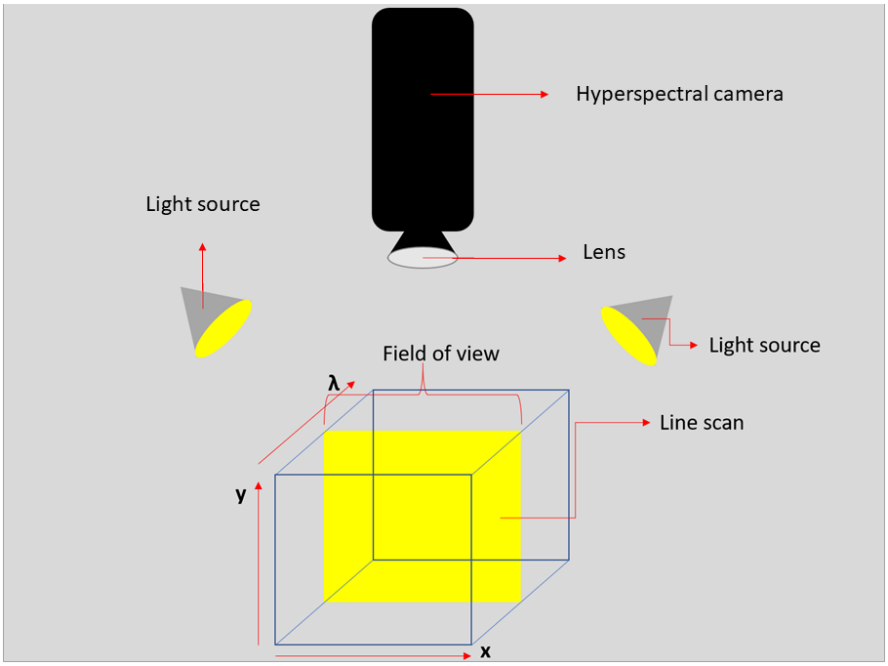

Figure 2.1 Line scan or push broom scanning method

2.6.1.1 Unsupervised and supervised classification models

Qualitative and quantitative information can be extracted from hypercubes using exploratory data analysis. Since hyperspectral images contain high data dimension, it is imperative to present the data efficiently by reducing the excess data. Multivariate analysis uses data dimension reduction technique to analyse data covariance structure. Principal component analysis (PCA) is a data transformation technique that converts the dataset into linear combination of variables in smaller dimension that are not correlated with one another. It is the primary step in identifying important wavelengths by reducing the substantial amount of data. It is generally used for dimensionality reduction and outlier exclusion of data. Original dataset is transformed into principal components by orthogonal linear transformation; hence it is an unsupervised classification model. Partial Least Square Discriminant Analysis (PLS-DA) is a supervised classification model that uses orthogonal latent variables (a set of new variables). Latent variables are found by considering the covariance between response variables and design matrix. PLS-DA combines regression model (PLS) and classification model i.e., discriminant analysis

(DA) to assign a dataset in one of the previously created categories and thus becoming a robust technique.

2.6.1.2 Application of hyperspectral imaging and spectroscopy in flours

For food safety and quality assessment, today's food industry is moving towards rapid non-invasive techniques such as hyperspectral imaging. Studies have shown that hyperspectral imaging can be used to detect adulteration/contamination in foods with minimal sample preparation. For instance, contaminants such as melamine in non-fat and whole milk powder could be quantified by combining NIR hyperspectral imaging (970 to 1770 nm) with simple band ratio (Huang et al. 2016; Lim et al. 2016). Similarly, Liu et al. (2016) detected dicyandiamide in milk powder and quantified the adulterant in the range 405 to 970 nm using partial least square (PLS), least square support vector machine (LS-SVM), and back propagation neural network (BPNN) models.

In case of cereals, the use of Vis-NIR hyperspectral imaging has been widely explored in adulterated wheat flours. Researchers have detected and quantified traces of peanut and walnut powders in whole wheat flour using NIRS and hyperspectral imaging (Mishra et al. 2015; Zhao et al. 2019, 2018). Similarly, wheat flour adulterated with different concentrations of cereal flour adulterants such as sorghum, oat, and corn flours were detected in the range of 400 to 1000 nm (Verdú et al. 2016). On the other hand, successful characterization of heat-treated oat and wheat flour at various heating times and temperatures was carried out for bread making process in the wavelength range of 400 to 1000 nm (Verdú et al. 2016; Verdú et al. 2017). Su and Sun (2017) reported that organic wheat flour (Avatar variety, Ireland) adulterated with cassava flour and corn flour were easier to detect than the organic wheat flour adulterated with whole wheat flour in the range 897 to 1153 nm. In addition to these studies, researchers have detected the ergot bodies, fusarium infection, and mycotoxin content in wheat flour (Alisaac et al. 2019; Vermeulen et al. 2017). From the aforementioned studies, it can be concluded that hyperspectral imaging has the potential to be used for classifying flours that are adulterated or blended.

2.7 Scanning electron microscopy

Scanning electron microscope (SEM) is the most commonly used electron microscope for studying morphological features and component separation. The topography, morphology, and chemical composition of a sample can be obtained using SEM. The instrument operates under high vacuum condition where material surface is scanned at greater field-of-depth to obtain the microstructure of the sample with high resolution. In SEM, electrons are used as a source of illumination to increase resolution due to the shorter wavelengths of the electrons. Secondary electrons are generated when the incoming electrons collide with the loosely bonded outer electrons. They have low energy (10 to 50 eV) and affect the topographic contrast of the sample. SE production is determined by angle of incidence between the beam and the sample. Back scattered electrons are high energy electrons generated by the elastic collision between beam electrons and nuclei of atoms in specimen. Topographic contrast of the sample is accomplished by secondary electrons whereas back scattered electrons are used for illustrating contrast in elemental composition of the sample.

The SEM apparatus constitutes an electron gun, to generate electron beam, and several electromagnetic lenses including condenser, objective lenses, detector, and apertures. The electron gun can be either thermionic or field emission, where field emission gun has high beam brightness. In thermionic gun, a heating solid emits electrons whereas in the field emission gun, electrons are emitted in strong electric field. The electromagnetic lens is made of an iron pole piece comprising of a copper coil wire. The commonly used detector is Everhart-Thornley detector (E-T detector). In E-T detector, a high voltage (10 kV) is applied to the secondary electron detector coated with a scintillator. Secondary electron hits the scintillator with high voltage and generates light. Light converts into amplified electrons to produce electric signals. A magnetic field is generated when current is passed through a copper coil which converges the electron beam. The electron beam interacts with the sample and emits electrons or photons, which are collected at the detector. An SEM image (or micrograph) is produced by focussing the electron beam over a surface area of the specimen. Digital images are produced in the SEM where each image is digitized and saved as a digital file for every single scan. The advantage of digital scan is that it reduces the background noise effectively by taking an average of the multiple scans for the same area.

Some of the important parameters, which affect the image are accelerating voltage (kV), probe convergence angle (α), probe current (i), probe diameter or spot size (d), and working distance (WD). The probe diameter is given by,

$$d = \sqrt{\frac{4i}{\beta\pi^2\alpha^2}}$$

where i is the probe current, β is the beam brightness, and α is the probe convergence angle.

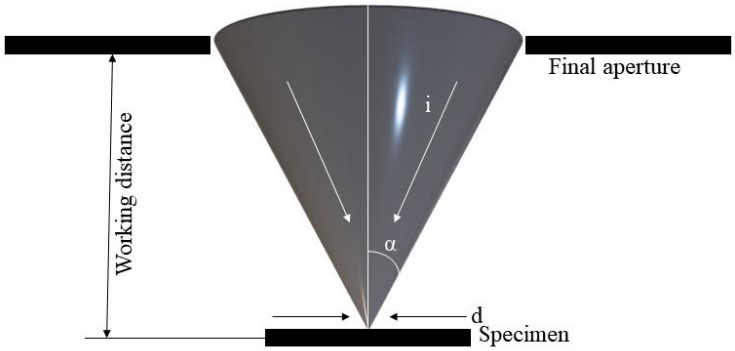

Figure 2.2 Relationship between the probe diameter, convergence angle, and working distance.

Resolution is the smallest distance between two points that can be resolved. High resolution is obtained by minimizing the probe size as cross-section diameter determines the resolution. Magnification is the ratio of scanned line length in the image displayed to the scanned line length on the specimen. Depth of field is the depth range of the focused image. It is increased by decreasing aperture size, magnification, and increasing working distance. Astigmatism occurs when images distort in different directions due to defocusing of not perfect cylindrical lenses. Surface charging of sample happens when non-conductive samples such as biological materials, produces a positive charge on the surface of the specimen that produces distorted images. Charging can be prevented by surface coating of specimen with a thin layer of highly conductive samples such as gold-palladium mixture or carbon, observing the specimen at low kV or low vacuum or Environmental Scanning Electron Microscopy (ESEM) observation, and using low voltage ion gun.

2.7.1 Application of scanning electron microscopy

SEM has been widely used to study the shape, size, structure, and surface morphology of food materials. Bhattacharya et al. (2005) reported microstructural changes in whole lentils *(Lens esculenta)* at different moisture contents using SEM images. They reported that the thickness of the outer seed coat varied from 25 to 65 µm in ellipsoid shape. Johnson et al. (2015) observed swelling of starch matrix in red and green lentils after cooking and cooling process. They reported that the deformation of structural changes was higher in cooled starches than in cooked starches especially, in green lentils. Similarly, Ahmed et al. (2016) used SEM to analyse the structure of lentil starch granules after pressure treatment. They reported that the starch granules retained their granular shape with smooth surfaces and change in surface with cracks for the pressure treatment of 500 MPa and 600 MPa, respectively. Miranda et al. (2019) used SEM to observe the different starches in bean varieties and changes occurred in the starch matrix due to gelatinization. SEM has been used to study the purity of starch granules after alkaline extraction (Lee et al. 2007).

Studies have shown the importance of starch-protein matrix separation using SEM (Assatory et al. 2019; Pelgrom et al. 2015; Schutyser et al. 2015). Cloutt et al. (1987) stated the significance of the size of starch granule in the separation of the starch-protein matrix in their air classification study of pulse flours. Similarly, (Pelgrom, Boom, et al. 2015) reported that larger starch granules enter the fine fraction by lowering the protein content of chickpea flours. Li et al. (2019) used SEM to characterize and compare the starches from pea, lentil, and faba bean with commercial starches. They found that the starches obtained from air-classified flours showed broken granules and scratches, whereas the commercial pea starch obtained from wet method had no such features. The damaged starch granules from the lentil starches were similar to damaged starch granules obtained from the commercial pea starches.

2.8 Research gap

To summarize, milling affects the particle size distribution and cell components, consequently affecting the chemical composition and microstructural properties of flour. There seem to be no studies to the best of our knowledge where non-destructive analysis techniques like hyperspectral

imaging and scanning electron microscopy have been used to study and compare milling of multiple pulse flours obtained from different mills. Therefore, the main aim of this research is to characterize the four different types of pulse flours namely chickpea, navy bean, green lentil, and yellow pea flours, milled using Ferkar and roller mills. The individual objectives are stated in chapter 1.

References

Abdel-Rahman, E.-S. A., F. A. El-Fishawy, M. A. El-Geddawy, T. Kurz, and M. N. El-Rify. 2007. The Changes in the Lipid Composition of Mung Bean Seeds as Affected by Processing Methods. *International Journal of Food Engineering* 3(5). https://doi.org/doi:10.2202/1556-3758.1186.

Adsule, R. N., S. S. Kadam, D. K. Salunkhe, and B. S. Luh. 1986. Chemistry and technology of green gram (Vigna radiata [L.] Wilczek). *C R C Critical Reviews in Food Science and Nutrition* 25(1):73–105. https://doi.org/10.1080/10408398609527446.

Alisaac, E., J. Behmann, A. Rathgeb, P. Karlovsky, H. W. Dehne, and A. K. Mahlein. 2019. Assessment of fusarium infection and mycotoxin contamination of wheat kernels and flour using hyperspectral imaging. *Toxins* 11(10):1–18. https://doi.org/10.3390/toxins11100556.

Anton, A. A., K. A. Ross, O. M. Lukow, R. G. Fulcher, and S. D. Arntfield. 2008. Influence of added bean flour (Phaseolus vulgaris L.) on some physical and nutritional properties of wheat flour tortillas. *Food Chemistry* 109(1):33–41. https://doi.org/10.1016/j.foodchem.2007.12.005.

Aparecida Tavares de Miranda, J., L. Maria Jaeger de Carvalho, I. Miranda de Castro, J. Luiz Viana de Carvalho, A. Luiz de Alcântara Guimarães, and A. Cláudia de Macêdo Vieira. 2019. Starch Granules from Cowpea, Black, and Carioca Beans in Raw and Cooked Forms. *Legume Crops* 2061:1–7. https://doi.org/10.5772/intechopen.85656.

Assatory, A., M. Vitelli, A. R. Rajabzadeh, and R. L. Legge. 2019. Dry fractionation methods for plant protein, starch and fiber enrichment: A review. *Trends in Food Science and Technology* 86(February):340–351. https://doi.org/10.1016/j.tifs.2019.02.006.

Barakoti, L. and K. Bains. 2007. Effect of household processing on the in vitro bioavailability of iron in mungbean (Vigna radiata). *Food and Nutrition Bulletin* 28(1):18–22. https://doi.org/10.1177/156482650702800102.

Bazaz, R., W. N. Baba, F. A. Masoodi, and S. Yaqoob. 2016. Formulation and characterization of hypo allergic weaning foods containing potato and sprouted green gram. *Journal of Food Measurement and Characterization* 10(3):453–465. https://doi.org/10.1007/s11694-016-9324-1.

Bellido, G. G. 2002. Effects of pre-treatment and micronization on the cookability, chemical components and physical structure of navy and black beans (Phaseolus vulgaris L.). Unpublished M.Sc. thesis. Winnipeg, MB: Department of Food Science, University of Manitoba.

Bhattacharya, S., H. V. Narasimha, and S. Bhattacharya. 2005. The moisture dependent physical and mechanical properties of whole lentil pulse and split cotyledon. *International Journal of Food Science and Technology* 40(2):213–221. https://doi.org/10.1111/j.1365-2621.2004.00933.x

Bourré, L., P. Frohlich, G. Young, Y. Borsuk, E. Sopiwnyk, A. Sarkar, … L. Malcolmson. 2019. Influence of particle size on flour and baking properties of yellow pea, navy bean, and red lentil flours. *Cereal Chemistry* 96(4):655–667. https://doi.org/10.1002/cche.10161.

Campbell, G. M. (2007). Chapter 7 Roller Milling of Wheat. *Handbook of Powder Technology*, *12*, 383–419. https://doi.org/10.1016/S0167-3785(07)12010-8.

Chan, Y. S., Zhang, Y., Sze, S. C. W., and Ng, T. B. 2014. A thermostable trypsin inhibitor with antiproliferative activity from small pinto beans. *Journal of Enzyme Inhibition and Medicinal Chemistry* 29(4):485–490. https://doi.org/10.3109/14756366.2013.805756.

Cloutt, P., A. F. Walker, and D. J. Pike. 1987. Air classification of flours of three legume species: Fractionation of protein. *Journal of the Science of Food and Agriculture* 38(2):177–186. https://doi.org/10.1002/jsfa.2740380209.

Dahiya, P. K., A. R. Linnemann, M. A. J. S. Van Boekel, N. Khetarpaul, R. B. Grewal, and M. J. R. Nout. 2015. Mung Bean: Technological and Nutritional Potential. *Critical Reviews in Food Science and Nutrition* 55(5):670–688. https://doi.org/10.1080/10408398.2012.671202

Dahl, W. J., L. M. Foster, and R. T. Tyler. 2012. Review of the health benefits of peas (Pisum sativum L.). *British Journal of Nutrition 108*(SUPPL. 1). https://doi.org/10.1017/S0007114512000852.

Dai, J., and R. J. Mumper. 2010. Plant phenolics: Extraction, analysis and their antioxidant and anticancer properties. *Molecules 15*(10):7313–7352. https://doi.org/10.3390/molecules15107313.

ElMasry, G., M. Kamruzzaman, D. W. Sun, and P. Allen. 2012. Principles and Applications of Hyperspectral Imaging in Quality Evaluation of Agro-Food Products: A Review. *Critical*

Reviews in Food Science and Nutrition 52(11):999–1023. https://doi.org/10.1080/10408398.2010.543495.

ElMasry, G., and W.D. Sun. 2010. Principles of Hyperspectral imaging technology. *Hyperspectral Imaging for Food Quality Analysis and Control*, ed. Da-Wen Sun, 3-45. London, UK: Academic press.

Fernández Pierna, J. A., P. Vermeulen, O. Amand, A. Tossens, P. Dardenne, and V. Baeten. 2012. NIR hyperspectral imaging spectroscopy and chemometrics for the detection of undesirable substances in food and feed. *Chemometrics and Intelligent Laboratory Systems* 117:233–239. https://doi.org/10.1016/j.chemolab.2012.02.004.

Fiona S. Atkinson, Kaye Foster-Powell, and Jennie C. Brand-Miller. 2008. International Table of Glycemic Index and Glycemic Load values. *Diabetes Care* 31(12):2281–2283.

Gujska, E., D.Reinhard, And K. Khan. 1994. Physicochemical Properties of Field Pea, Pinto and Navy Bean Starches. *Journal of Food Science* 59(3): 634–636. https://doi.org/10.1111/j.1365-2621.1994.tb05580.x.

Han, J. (Jay), J. A. M. Janz, and M. Gerlat. 2010. Development of gluten-free cracker snacks using pulse flours and fractions. *Food Research International* 43(2):627–633. https://doi.org/10.1016/j.foodres.2009.07.015.

Harina,T. H. and D. A. Ramirez. 1978. The amount and distribution of carotenoids in the mungbean seed (Vigna radiata Wilczek). *Philippine Journal of Crop Science* 3(2):65–70.

Hossain, Z., X. Wang, C. Hamel, J. Diane Knight, M. J. Morrison, and Y. Gan. 2016. Biological nitrogen fixation by pulse crops on semiarid Canadian prairies. *Canadian Journal of Plant Science* 97(1):119–131. https://doi.org/10.1139/cjps-2016-0185.

Huang, M., M. S. Kim, S. R. Delwiche, K. Chao, J. Qin, C. Mo, … and Q. Zhu. 2016. Quantitative analysis of melamine in milk powders using near-infrared hyperspectral imaging and band ratio. *Journal of Food Engineering* 181:10–19. https://doi.org/10.1016/j.jfoodeng.2016.02.017.

Hulse, J. H. 1991. Uses of Tropical Grain Legumes. *In proceedings of a Consultants Meeting in ICRISAT (International Crops Research Institute for the Semi -Arid Tropics)* 27-30 Mar 1989 ICRISAT Center, India. Patancheru A.P. 502 324.

Imtiaz H. 2007. Evaluation of weaning foods formulated from germinated wheat and mungbean from Bangladesh. *African Journal of Food Science* 5(17):897–903. https://doi.org/10.5897/ajfs11.180.

Jain, A. K., S. Kumar, and J. D. S. Panwar. 2009. Antinutritional Factors and Their Detoxification in Pulses- a Review. *Agricultural Reviews* 30(1):64–70.

Johnson, C. R., D. Thavarajah, P. Thavarajah, S. Payne, J. Moore, and J. B. Ohm. 2015. Processing, cooking, and cooling affect prebiotic concentrations in lentil (lens culinaris medikus). *Journal of Food Composition and Analysis* 38:106–111. https://doi.org/10.1016/j.jfca.2014.10.008.

Johnson, S. K., S. J. Thomas, and R. S. Hall. 2005. Palatability and glucose, insulin and satiety responses of chickpea flour and extruded chickpea flour bread eaten as part of a breakfast. *European Journal of Clinical Nutrition* 59(2):169–176. https://doi.org/10.1038/sj.ejcn.1602054.

Jukanti, A. K., P. M. Gaur, C. L. L. Gowda, and R. N. Chibbar. 2012. Nutritional quality and health benefits of chickpea (Cicer arietinum L.): A review. *British Journal of Nutrition* 108(SUPPL. 1). https://doi.org/10.1017/S0007114512000797.

Kaack, K., and L. Pedersen. 2005. Low energy chocolate cake with potato pulp and yellow pea hulls. *European Food Research and Technology* 221(3–4):367–375. https://doi.org/10.1007/s00217-005-1181-9.

Kasemsuwan, T., T. Bailey, and J. Jane. 1998. Preparation of clear noodles with mixtures of tapioca and high-amylose starches. *Carbohydrate Polymers* 36(4):301–312. https://doi.org/10.1016/S0144-8617(97)00256-7.

Lee, H. C., A. K. Htoon, and J. L. Paterson. 2007. Alkaline extraction of starch from Australian lentil cultivars Matilda and Digger optimised for starch yield and starch and protein quality. *Food Chemistry* 102(3):551–559. https://doi.org/10.1016/j.foodchem.2006.03.042.

Li, L., Yuan, Setia T. Z., R. B. Raja, B. Zhang, and Y. Ai. 2019. Characteristics of pea, lentil and faba bean starches isolated from air-classified flours in comparison with commercial starches. *Food Chemistry*, 276(September 2018):599–607. https://doi.org/10.1016/j.foodchem.2018.10.064.

Lim, J., G. Kim, C. Mo, M. S. Kim, K. Chao, J. Qin, … B. K. Cho. 2016. Detection of

melamine in milk powders using near-infrared hyperspectral imaging combined with regression coefficient of partial least square regression model. *Talanta* 151:183–191. https://doi.org/10.1016/j.talanta.2016.01.035.

Liu, C., W. Liu, J. Yang, Y. Chen, and L. Zheng. 2016. Non-destructive detection of dicyandiamide in infant formula powder using multi-spectral imaging coupled with chemometrics. *Journal of the Science of Food and Agriculture* 97(7):2094–2099. https://doi.org/10.1002/jsfa.8014.

Maskus, H., L. Bourré, S. Fraser, A. Sarkar, and L. Malcolmson. 2016. Effects of grinding method on the compositional, physical, and functional properties of whole and split yellow pea flours. *Cereal Foods World* 61(2):59–64. https://doi.org/10.1094/CFW-61-2-0059.

McGoverin, C. M., P. Engelbrecht, P. Geladi, and M. Manley. 2011. Characterisation of non-viable whole barley, wheat and sorghum grains using near-infrared hyperspectral data and chemometrics. *Analytical and Bioanalytical Chemistry 401*(7):2283–2289. https://doi.org/10.1007/s00216-011-5291-x.

Megan A. McCrory, Bruce R. Hamaker, Jennifer C. Lovejoy, and P. E. E. 2010. Pulse Consumption, Satiety, and Weight Management. *American Society for Nutrition. Advances in Nutrition* 1:17–30. https://doi.org/10.3945/an.110.1006.1.

Miñarro, B., E.Albanell, N. Aguilar, B. Guamis, and M. Capellas. 2012. Effect of legume flours on baking characteristics of gluten-free bread. *Journal of Cereal Science* 56(2):476–481. https://doi.org/10.1016/j.jcs.2012.04.012.

Mishra, P., A. Herrero-Langreo, P. Barreiro, J. M. Roger, B. Diezma, N. Gorretta, and L. Lleó. 2015. Detection and quantification of peanut traces in wheat flour by near infrared hyperspectral imaging spectroscopy using principal-component analysis. *Journal of Near Infrared Spectroscopy* 23(1):15–22. https://doi.org/10.1255/jnirs.1141.

Mubarak, A. E. 2005. Nutritional composition and antinutritional factors of mung bean seeds (Phaseolus aureus) as affected by some home traditional processes. *Food Chemistry* 89(4): 489–495. https://doi.org/10.1016/j.foodchem.2004.01.007.

Nayak, B., J. D. J. Berrios, J. R. Powers, and J. Tang. 2011. Effect of Extrusion on the Antioxidant Capacity and Color Attributes of Expanded Extrudates Prepared from Purple Potato and Yellow Pea Flour Mixes. *Journal of Food Science* 76(6):874–883.

https://doi.org/10.1111/j.1750-3841.2011.02279.x.

Noor Aziah, A. A., A. Y. Mohamad Noor and L.H. Ho. 2012. Physicochemical and organoleptic properties of cookies incorporated with legume flours. *International Food Research Journal* 19(4):1539–1543. Retrieved from http://www.ifrj.upm.edu.my/19 (04) 2012/34 IFRJ 19 (04) 2012 Noor Aziah (385).pdf.

Osorio-Díaz, P., E. Agama-Acevedo, M. Mendoza-Vinalay, J. Tovar, and L. A. Bello-Pérez. 2008. Pasta added with chickpea flour: Chemical composition, in vitro starch digestibility and predicted glycemic index. *Ciencia y Tecnologia Alimentaria* 6(1):6–12. https://doi.org/10.1080/11358120809487621.

Dahiya P. K., A. R. Linnemann, M. A. J. S. Van Boekel, N. Khetarpaul, R. B. Grewal, M. J. R. N. 2015. Mung Bean: Technological and Nutritional Potential. *Critical Reviews in Food Science and Nutrition* 55(5):670–688.

Pasha, I., S. Rashid, F. M. Anjum, M. T. Sultan, M. M. Nasir Qayyum, and F. Saeed. 2011. Quality evaluation of wheat-mungbean flour blends and their utilization in baked products. *Pakistan Journal of Nutrition* 10(4):388–392. https://doi.org/10.3923/pjn.2011.388.392.

Pelgrom, P. J. M., R. M. Boom, and M. A. I. Schutyser. 2015. Method Development to Increase Protein Enrichment During Dry Fractionation of Starch-Rich Legumes. *Food and Bioprocess Technology* 8(7):1495–1502. https://doi.org/10.1007/s11947-015-1513-0.

Pelgrom, P. J. M., A. M. Vissers, R. M. Boom, and M. A. I. Schutyser. 2013. Dry fractionation for production of functional pea protein concentrates. *Food Research International* 53(1): 232–239. https://doi.org/10.1016/j.foodres.2013.05.004.

Rachwa-Rosiak, D., E. Nebesny, and G. Budryn. 2015. Chickpeas—Composition, Nutritional Value, Health Benefits, Application to Bread and Snacks: A Review. *Critical Reviews in Food Science and Nutrition* *55*(8):1137–1145. https://doi.org/10.1080/10408398.2012.687418.

Rizkalla, S. W., F. Bellisle, and G. Slama. 2002. Health benefits of low glycaemic index foods, such as pulses, in diabetic patients and healthy individuals. *British Journal of Nutrition*, 88(S3):255–262. https://doi.org/10.1079/bjn2002715.

Sakhare, S. D., A. A.Inamdar, S. B. Gaikwad, D, I., and G, V. R. 2014. Roller milling fractionation of green gram (Vigna radiata): optimization of milling conditions and

chemical characterization of millstreams. *Journal of Food Science and Technology* 51(12):3854–3861. https://doi.org/10.1007/s13197-012-0903-9.

Scanlon, M. G., S. Thakur, R. T. Tyler, A. Milani, T. Der, and J. Paliwal. 2018. The critical role of milling in pulse ingredient functionality. *Cereal Foods World* 63(5):201–206. https://doi.org/10.1094/CFW-63-5-0201.

Schutyser, M. A. I., P. J. M. Pelgrom, A. J. van der Goot, and R. M. Boom. 2015. Dry fractionation for sustainable production of functional legume protein concentrates. *Trends in Food Science and Technology* 45(2):327–335. https://doi.org/10.1016/j.tifs.2015.04.013.

Singh, M., J. A. Byars, and S. X. Liu. 2015. Navy Bean Flour Particle Size and Protein Content Affect Cake Baking and Batter Quality1. *Journal of Food Science* 80(6):E1229–E1234. https://doi.org/10.1111/1750-3841.12869.

Su, W. H., and D. W. Sun. 2017. Evaluation of spectral imaging for inspection of adulterants in terms of common wheat flour, cassava flour and corn flour in organic Avatar wheat (Triticum spp.) flour. *Journal of Food Engineering* 200:59–69. https://doi.org/10.1016/j.jfoodeng.2016.12.014.

Su, W. H., and D. W. Sun. 2018. Fourier Transform Infrared and Raman and Hyperspectral Imaging Techniques for Quality Determinations of Powdery Foods: A Review. *Comprehensive Reviews in Food Science and Food Safety* 17(1):104–122. https://doi.org/10.1111/1541-4337.12314.

Tang, D., Y. Dong, H. Ren, L. Li, and C. He. 2014. A review of phytochemistry, metabolite changes, and medicinal uses of the common food mung bean and its sprouts (Vigna radiata). *Chemistry Central Journal* 8(1):1–9. https://doi.org/10.1186/1752-153X-8-4.

Thakur, S., M. G. Scanlon, R. T. Tyler, A. Milani, and J. Paliwal. 2019. Pulse Flour Characteristics from a Wheat Flour Miller's Perspective: A Comprehensive Review. *Comprehensive Reviews in Food Science and Food Safety* 18(3):775–797. https://doi.org/10.1111/1541-4337.12413

Verdú, S., E. Ivorra, A. J. Sánchez, J. M. Barat, and R. Grau. 2016. Spectral study of heat treatment process of wheat flour by VIS/SW-NIR image system. *Journal of Cereal Science* 71:99–107. https://doi.org/10.1016/j.jcs.2016.08.008.

Verdú, S., F. Vásquez, R. Grau, E. Ivorra, A. J. Sánchez, and J. M. Barat. 2016. Detection of

adulterations with different grains in wheat products based on the hyperspectral image technique: The specific cases of flour and bread. *Food Control* 62:373–380. https://doi.org/10.1016/j.foodcont.2015.11.002.

Verdú, S., F. Vásquez, E. Ivorra, A. J. Sánchez, J. M. Barat, and R. Grau. 2017. Hyperspectral image control of the heat-treatment process of oat flour to model composite bread properties. *Journal of Food Engineering* 192:45–52. https://doi.org/10.1016/j.jfoodeng.2016.07.017.

Vermeulen, P., M. B. Ebene, B.Orlando, J. A.Fernández Pierna, and V. Baeten. 2017. Online detection and quantification of particles of ergot bodies in cereal flour using near-infrared hyperspectral imaging. *Food Additives and Contaminants - Part A Chemistry, Analysis, Control, Exposure and Risk Assessment* 34(8):1312–1319. https://doi.org/10.1080/19440049.2017.1336798.

Wang, N., P. R. Bhirud, F. W. Sosulski, and R. T. Tyler. 1999. Pasta-like product from pea flour by twin-screw extrusion. *Journal of Food Science* 64(4):671–678. https://doi.org/10.1111/j.1365-2621.1999.tb15108.x.

Yamsaengsung, R., R. Schoenlechner, and E. Berghofer. 2010. The effects of chickpea on the functional properties of white and whole wheat bread. *International Journal of Food Science and Technology* 45(3):610–620. https://doi.org/10.1111/j.1365-2621.2009.02174.x.

Zhao, X., W. Wang, X. Ni, X. Chu, Y. F. Li, and C. Lu. 2019. Utilising near-infrared hyperspectral imaging to detect low-level peanut powder contamination of whole wheat flour. *Biosystems Engineering* 184:55–68. https://doi.org/10.1016/j.biosystemseng.2019.06.010.

Zhao, X., W. Wang, X. Ni, X. Chu, Y. F. Li, and C. Sun. 2018. Evaluation of near-infrared hyperspectral imaging for detection of peanut and walnut powders in whole wheat flour. *Applied Sciences (Switzerland) 8*(7). https://doi.org/10.3390/app8071076.

Zia-Ul-Haq, M., S. Iqbal, S. Ahmad, M.Imran, A. Niaz, and M. I. Bhanger. 2007. Nutritional and compositional study of Desi chickpea (Cicer arietinum L.) cultivars grown in Punjab, Pakistan. *Food Chemistry* 105(4):1357–1363. https://doi.org/10.1016/j.foodchem.2007.05.004.

CHAPTER 3. Classification of pulse flours using near infrared hyperspectral imaging

This chapter is based on the manuscript submitted in the journal "LWT- Food Science and Technology" entitled 'Classification of pulse flours using near infrared spectroscopy and hyperspectral imaging'.

3.1 Abstract

With increasing consumer interest in healthy food formulations made from pulse flours, the research gap in characterizing them based on their pulse-type and milling technique has come to the limelight. To this end, the feasibility of using hyperspectral imaging in the visible near infrared (Vis-NIR) (400 to 1000 nm) and short wave infrared (SWIR) (1000 to 2500 nm) regions to classify pulse flours (viz. chickpea, yellow pea, navy bean and green lentil) based on the pulse-type and milling methods were investigated. Unsupervised and supervised classification models were developed for preprocessed data using unsupervised principal component analysis (PCA) and supervised partial least squares discriminant analysis (PLS-DA), respectively. This multivariate exploration of data established that supervised classification for pulse flour type could be done with 100% accuracy in the Vis-NIR wavelength range of 530 to 700 nm, which primarily exploited the color attributes of the flour samples. For milling method-based classification, PLS-DA models developed using SWIR regions of 1370 to 1500 nm and 1700 to 2000 nm played a significant role in discriminating the flour samples yielded 95% classification accuracy. These regions are associated with the O-H and N-H overtones of the proteins found in flour samples. It can be deduced from the study that hyperspectral imaging in the range of 400 to 2500 nm combined with multivariate data classification methods can reliably be used by the food industry for the characterization of pulse flours.

Keywords: pulses, flours, spectra, pixels, classification, PLS-DA

3.2 Highlights

1. Wavelength region from 530 to 700 nm effectively classified pulse flour types

2. Protein linked wavelengths in SWIR region discriminated samples based on milling method

3. Supervised classification maps depicted accuracies in the range of 95 to 100%

4. Hyperspectral imaging is a reliable tool for pulse flour characterization

3.3 Introduction

As a rich source of protein, carbohydrates, minerals, vitamins, and fibre, the edible seeds of plants in the family *Fabaceae*, called pulses, form a nutritious traditional addition to the human diet. Increasing modern consumer demand for pulses has been achieved with non-traditional techniques such as incorporating pulse flours into conventional formulations that in past only contained wheat flour, e.g., breads, pasta, cookies, snack foods, etc. Considering that regular consumption of pulses either in whole or processed forms improves gut health and has a preventative effect on cardio-vascular diseases, cancer, and diabetes (Abdullah et al. 2017), palatability considerations such as texture, crunchiness, crispiness, etc. are particularly important to encourage the consumption of this healthy foodstuff.

Researchers have studied characteristics of red lentil flour extrudate, reporting that enhanced texture can be achieved through the adjustment of processing parameters (Guillermic et al.2021; Luo et al.2020). The suitability of a pulse flour for a specific end product also depends on flour parameters, such as starch damage, and protein quality. The milling method plays a significant role in characterizing pulse flours as it impacts these flour parameters. Flours appearing similar upon visual inspection may have different properties as a function of various milling techniques. Differences in protein content in flours produced from hammer mill, stone mill, pin mill, and roller mill have been reported (Maskus et al. 2016; Schutyser et al. 2015; Thakur et al. 2019). Blending the flours obtained from different mills changes their overall chemical composition and particle size distribution, which in turn affects the functional and nutritional properties of the flour, affecting the quality of the end products (Su and Sun 2018). Systematic studies for pulse flour characterization based on pulse type and milling method hold great significance to quality control; however, no standardized characterization of pulse flours exists.

Near-infrared spectroscopy (NIRS) is an established spectroscopic method to analyse food products. Combining hyperspectral imaging (HSI) with NIRS provides a detailed analysis of the nutritional profile and biochemical distributions within samples where the former gives the spatial information of the chemical constituents (ElMasry et al. 2012). NIRS and short wave infrared (SWIR) hyperspectral imaging integrated with multivariate data analysis techniques have been successfully implemented for the characterization of food products and raw materials (Babellahi et al. 2020; Chaudhry et al. 2018). These techniques are valuable in detecting and quantifying adulteration by determining the chemical composition of samples. Owing to the success of these techniques in unraveling the constitutional characteristics of agri-food materials, NIRS and HSI were employed to classify the flours based on pulse type and milling method for flour characterization.

More specifically in the present study, spectral profiles in the Vis-NIR region, NIR regions of hyperspectral images were investigated as means to classify flours of different pulse types (namely, chickpea, navy bean, green lentil, and yellow pea) that were milled using two different methods (i.e., single-stage Ferkar mill and multi-stage roller mill).

3.4 Materials and Methods

3.4.1 Sample preparation

Pulse samples in this study were procured from the 2018 growing season. The chickpeas (CDC Orion), green lentils (CDC Greenstar), and yellow peas (CDC Spectrum) were grown in Limerick, Saskatchewan, and the navy beans (Nautica) from Hensall, Ontario. The pulses were pre-broken using a hammer mill (Model 120-B, Jacobson Inc., Iowa, U.S.) with a screen size of 3.175 mm prior to milling and subsequently milled using a single-stage Ferkar mill (model: Ferkar 5; KFM, Slovenia) and a roller mill (Buhler, MLU 202 laboratory mill; Buhler Group, Switzerland) at the Canadian International Grains Institute (Cigi), Winnipeg, Manitoba. Three kilograms (kg) of whole pulses were milled using Ferkar mill utilizing a screen size of 0.140 mm (50 Hz motor and 8 Hz feed rate). In the case of roller mill, the three break rolls were set at B1 (0.1 mm), B2 (0.01 mm), and B3 (0.01 mm), and the three reduction rolls (1M, 2M, 3M) had a gap size of 0.01 mm. The feed rate in this case was 5 kg/hr.

3.4.2 Flour blends from roller mill

While milling, six flour streams were produced separately and recombined into flour blends. Combination of B1, B2, and B3 flours for all pulse-types were blended into break flours (named as B1+B2+B3). Similarly, a combination of 1M, 2M, and 3M flours for yellow pea and green lentil were blended into middling/reduction flours (named as 1M+2M+3M). In the case of chickpea and navy bean, there were two types of middling flour blends; one consisted of 1M flour (named as 1M) and the other was a blend of 2M and 3M flour streams (named as 2M+3M). A representative blend of B1, B2, B3, 1M, 2M, and 3M flour streams was combined to yield straight grade (SG) flour which was proportional to the yield of the milled product.

3.4.3 Hyperspectral imaging system

Hyperspectral images of the pulse flour samples were acquired using Vis-NIR and SWIR line-scanning HSI systems (SPECIM Spectral Imaging Ltd., Oulu, Finland). The Vis-NIR system consisted of a charge coupled device (CCD) camera that had a sensor array of 1024 × 896 pixels. The camera was equipped with a spectrograph (SPECIM V10E) operating in the wavelength range of 397.66 to 1003.81 nm with a spectral resolution of 2.6 nm and a focusing lens (SPECIM OLET 15). Two 150W tungsten lamps (3900-ER, Illumination Technology, Inc., USA) located on the two sides of the sample stage at 45˚ were used as illumination sources. The SWIR system consisted of a thermo-electrically cooled SWIR camera and a spectrograph (SPECIM N25E) that had a sensor array of 300 × 384 × 288 pixels with a cryogenically cooled mercury-cadmium-telluride (MCT) detector array. The image hypercubes were obtained in the wavelength range of 953.36-2567.37 nm with a spectral resolution of 5.6 nm and a 30 mm focusing lens (SPECIM OLES 30).

3.4.4 Image acquisition and correction

The systems were switched on 30 minutes prior to sample scanning to achieve thermal and temporal stability of the lighting system and camera (Castorena, Morrison, Paliwal, and Erkinbaev, 2015; Erkinbaev, Derksen, and Paliwal, 2019). For both the cameras, the frame rate was set at 20 frames per second (fps). To obtain the best aspect ratio of the frame rate and

exposure time, the speed of the moving stage was set at 7 mm/s for both systems (Erkinbaev et al. 2019). The exposure time was set at 20 ms for the Vis-NIR and 8 ms for the SWIR systems. To minimize the air exposure of the sample, the flours were kept in a sealed air-tight bags during handling and were taken out of the bag only for scanning. The shutter was closed automatically to obtain a black reference and a 99% Spectralon reflectance standard (Labsphere, North Sutton, NH) was positioned at the top of each image for white reference. Once the images were acquired, black and white reference corrections were applied.

The relative reflectance R, was calculated using the following equation,

$$R = \frac{H - D}{W - D}$$

where, H represents the original hyperspectral image; D and W represent the signals acquired for black and white references, respectively.

3.4.5 Image processing and spectra acquisition

For the classification of pulse-type and milling method, spectra-based and pixel-based approaches were followed. Prior to spectral extraction, the wavelengths with poor signal-to-noise-ration (SNR) at the two extremities of the spectra were removed from the hypercubes for both the Vis-NIR and SWIR ranges. This step was followed by delineation of an area of interest from the background using binary masks. The pixels of the sample images were allocated a value of 1 (white) and the pixels of the unwanted background were allocated a value of 0 (black). Four different binary masks (one for each pulse-type) were developed to separate pulses from the background. In case of the Vis-NIR range, the navy bean and chickpea flours showed the best contrast from the background at 526 nm and 634 nm, respectively. For green lentil and yellow pea flours, the binary masks were developed using images at 688 nm and 742 nm, respectively. For the SWIR range, binary masks for navy bean, chickpea, green lentil, and yellow pea flours were developed from the images at 2017 nm, 1625 nm, 1737 nm, and 1231 nm, respectively. After the implementation of binary masks, spectra were extracted from each pixel. A representative spectrum was generated by averaging the pixels in each image of the sample. In each case (Vis-NIR and SWIR range), the final dataset of 140 samples was formulated and

Kennard-stone algorithm was used for splitting the dataset into calibration (70%) and validation (30%). Figures 3.1a and 3.1b depict the Vis-NIR and SWIR spectra of the four pulse flours, respectively.

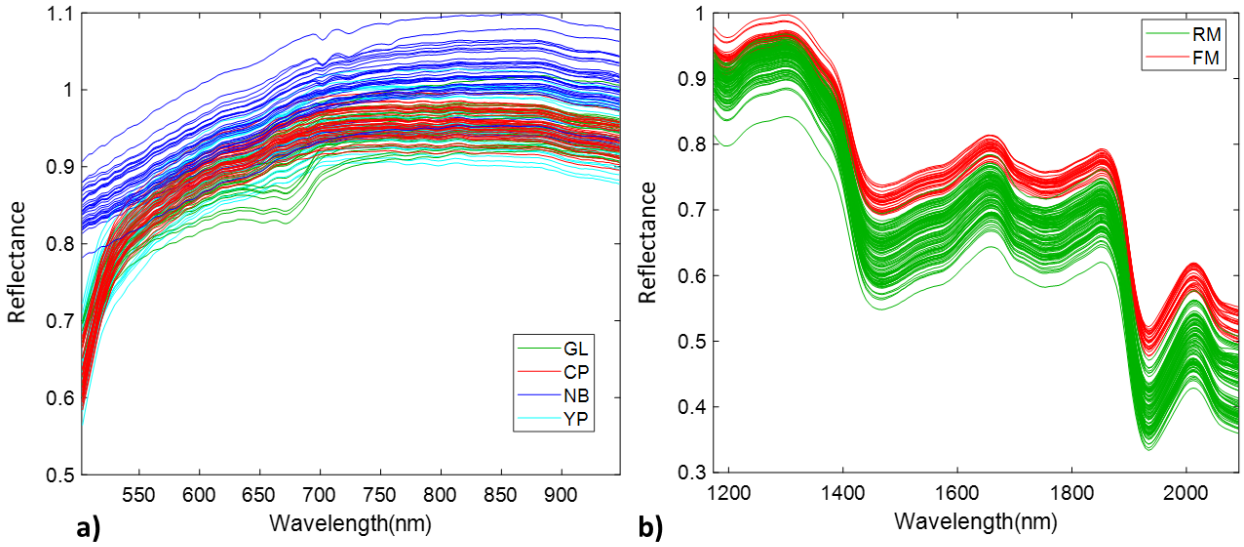

Figure 3.1 a) Vis-NIR spectra of green lentil (GL), chickpea (CP), navy bean (NB) and yellow pea (YP) flours b) SWIR spectra of roller milled (RM) and Ferkar milled (FM) flours.

3.4.6 Multivariate data analysis

Multivariate analysis techniques viz. principal component analysis (PCA) and partial least squares discriminant analysis (PLS-DA) were used for outlier exclusion, data dimension reduction and model development. PCA is a data transformation technique where a large number of correlated variables are transformed into a smaller set of uncorrelated orthogonal variables known as principal components (PCs). PLS-DA, on the other hand, is a supervised classification algorithm which uses latent variables (LVs) that are not orthogonal to each other. The LVs are

found by considering the covariance between response variables and a design matrix, which includes dummy variables indicating various classes in the dataset.

Prior to the application of these multivariate data analysis techniques, spectral datasets were preprocessed using mathematical pre-treatments such as mean centering, first derivative, second derivative, smoothing, standard normal variate (SNV), and their combinations. PCA models were developed using mean-centered data and PLS-DA models used combinations of pre-treatments. Another approach of pixel-based classification was also used for developing classification maps. With the pixel-based approach, multiple hyperspectral images were concatenated to formulate one image which was further thresholded using k-means clustering. The mathematical pre-treatments were applied by unfolding the images prior to model development in Hypertools V2.0 (Mobaraki and Amigo 2018).

3.5 Results and Discussions

3.5.1 PCA based unsupervised classification

3.5.1.1 Classification of pulse flours in the Vis-NIR range

Figure 3.2 shows the spectra-based PCA classification model with PC scores separated (by different shapes and colors) by pulse-type and milling method. The PCA model was applied to the dataset of 140 samples in the Vis-NIR range for the mean-centered data, resulting in five PCs that accounted for a total of 99.99% of the variance in the dataset. For pulse-type classification, figures 3.2a and 3.2b depict the sample scores and loadings plots for PC1 and PC4, respectively. Clear groupings based on the pulse-type were observed by plotting PC1 scores against PC4. PC4 showed clear groupings between yellow peas, green lentils, and chickpeas. On the other hand, PC1 axis clearly distinguished navy bean flours from the other three flour types. Observing the loading plots of PC1 and PC4, significant peaks were observed at 520 nm, 545 nm, and 670 nm that contributed towards the discrimination of flours.

For milling method-based classification, satisfactory groupings were observed by plotting PC2 against PC3 (Figure 3.2c). The highest percentage of variance was captured by PC1 (87.43%) followed by the rest of the four PCs in the wavelength range of 502 nm to 694 nm. The

wavelengths that contributed the most towards the discrimination of PC scores were 550 nm and 670 nm.

All these wavelength peaks in the Vis-NIR region are associated with the color attributes of the samples. Previous studies have shown that absorption bands within the region from 450 nm to 670 nm are predominantly responsible for chromophore transitions of food/agricultural matrices (Ambrose and Cho 2014; Mishra et al. 2015). Chromophores in flour/powdered samples are comprised of various aromatic ring compounds or conjugated bonds containing C=O and C=C organic molecules. Therefore, it can be inferred that classification based on pulse-type and milling method is due to the color differences among flours.

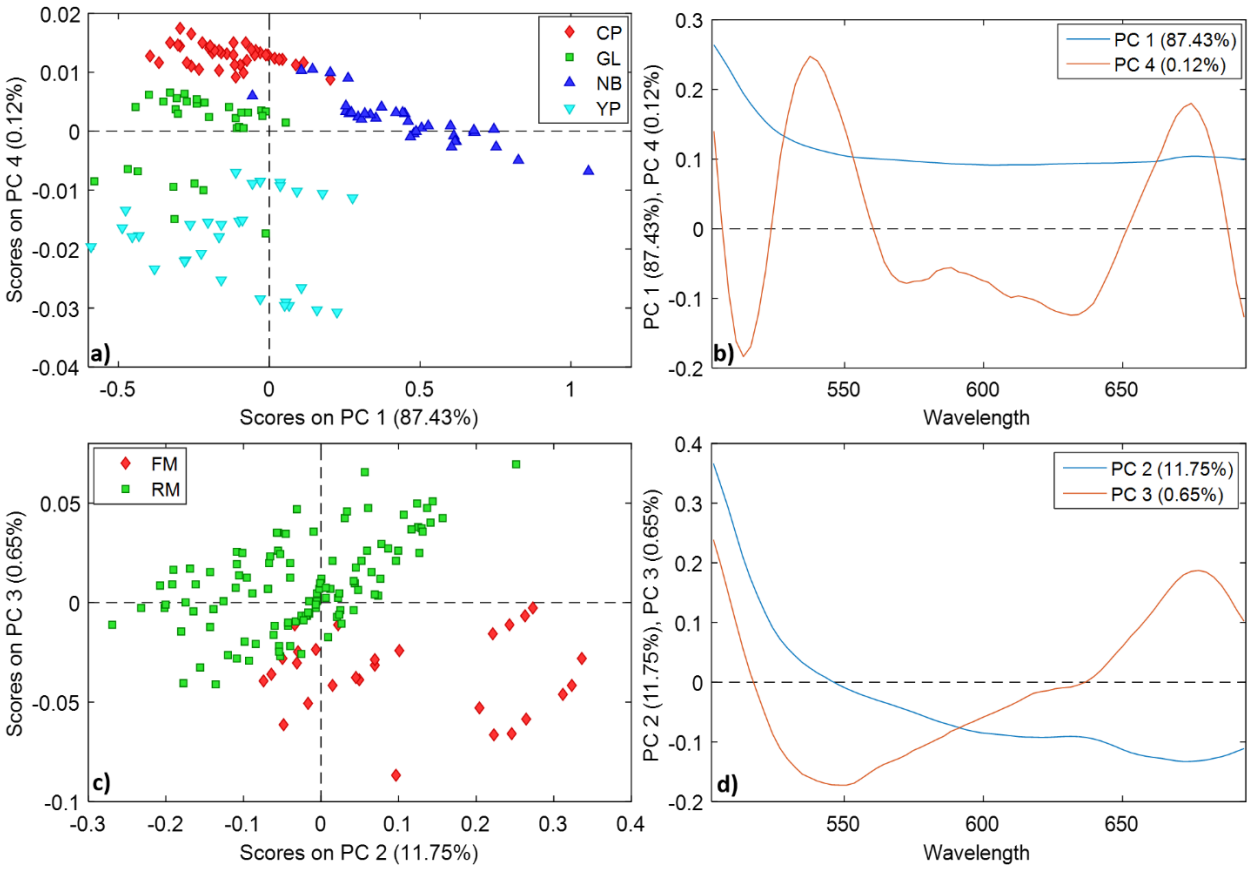

Figure 3.2 a) Scores plot of PC1 and PC4 separated by the pulse-type [CP = chickpea, GL = green lentil, NB = navy bean, YP = yellow pea] b) Loadings plot of PC1 and PC4 c) Scores plot

of PC2 and PC3 separated by the milling method [FM = Ferkar mill, RM = roller mill] d) Loadings plot of PC2 and PC3

Additionally, PCA was also applied on the pixels of the concatenated hyperspectral images in the wavelength range of 503 to 694 nm. Out of the 5 PCs, the first two explained 99.73% of the variance in the data. Clear groupings were observed on PC2 scores based on the pulse-type when the PC scores that were allocated to each pixel of the concatenated hyperspectral image (Figure 3.3). Based on the PC scores, the navy bean flour showed the best discrimination complementing the spectral-based PCA model where navy bean samples formulated a separate group. These groupings of flours can be due to color attributes, effectively discriminating them in the Vis-NIR region (Ambrose and Cho 2014).

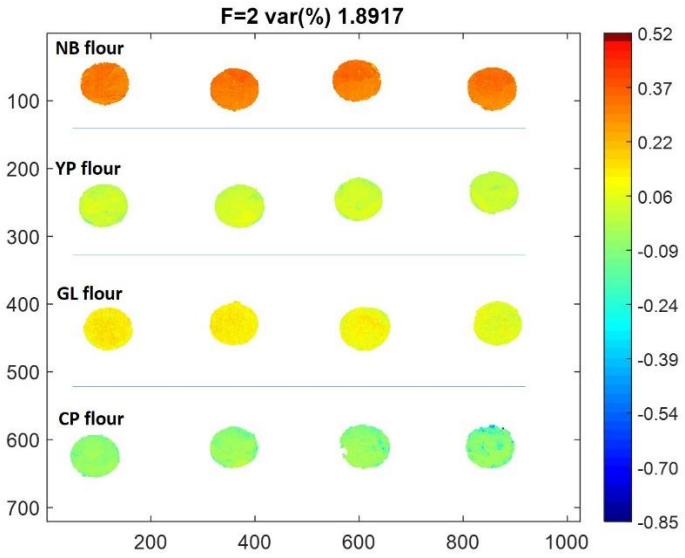

Figure 3.3 PC scores map for unsupervised classification based on pulse-type in the Vis-NIR region.

3.5.1.2 Classification of pulse flours in the SWIR range

For the spectra-based classification in the SWIR range (1173 to 2091 nm), the PCA model resulted in five PCs explaining a total of 99.97% of the total variance in the data. PC1 accounted for 97.24% of the variance and depicted clear groupings in PC scores based on the milling

method (Figure 3.4a). The loadings plot depicted 45 wavelengths (1200 to 1230 nm, 1350 to 1500 nm, and 1820 to 1865 nm) which significantly contributed towards the classification as shown in Figure 3.4b. The wavelength region from 1200 to 1230 nm is attributed to the first overtone of the C-H combination with a C-H structure. The C-H structure has a second overtone of C-H at 1225 nm. Similarly, the wavelength band absorption from the region 1820-1865 nm contributed to the second overtone of C=O stretch with a C-Cl structure at 1860 nm. A wide number of peaks were observed in the region from 1350 to 1500 nm (1395 nm, 1417 nm, 1440 nm, 1490 nm) which were related to the first overtones of C-H combination and O-H. The peaks arise due to the presence of the CH_2 structure (1395 and 1440 nm) and aromatic structure (1417 nm) of C-H combinations (Chen et al. 2013; Xiaobo 2010).

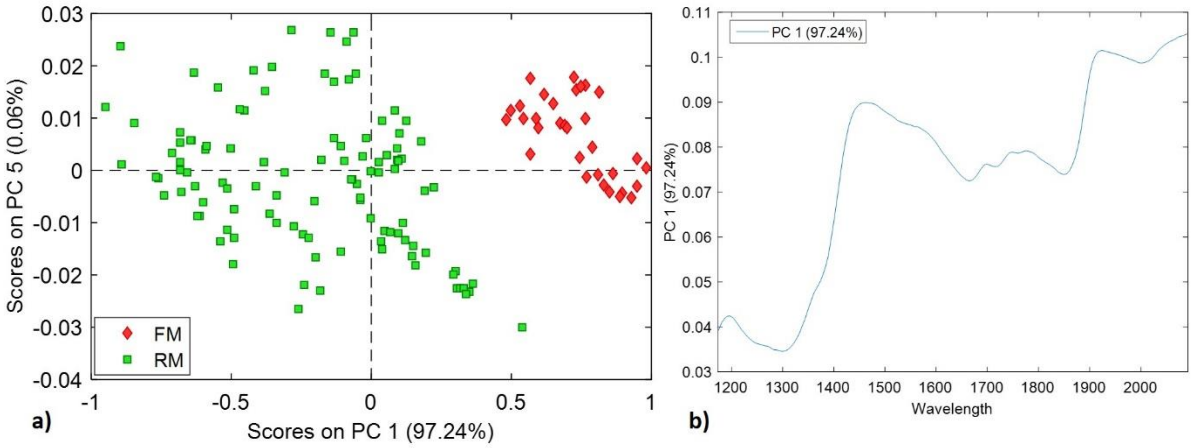

Figure 3.4 a) PC scores plot PC1 vs PC5 separated by milling method b) PC loadings plot for PC1 [FM = Ferkar mill, RM = roller mill]

Figure 3.5 shows 3-dimensional PC scores plots separated by pulse-type, milling method, milling streams, and protein content, respectively. In addition to the pulse-type and milling method-based classifications, a stream based classification (see Figure 3.5c) was also performed, but overall, the groupings were not encouraging. The PCA model showed clear distinction for chickpea flours, followed by navy bean and other flours in pulse-type-based classification. This can be due to the color difference and protein content (lowest compared to all other pulse flours) of the chickpea flours as depicted in Figure 3.5d. The classification can be better understood by comparing figures 3.5a to 3.5d that illustrate chickpea flours from the broken stream

(B1+B2+B3) and navy bean flour from the middling stream (2M+3M) possessed the lowest and highest protein contents, respectively.

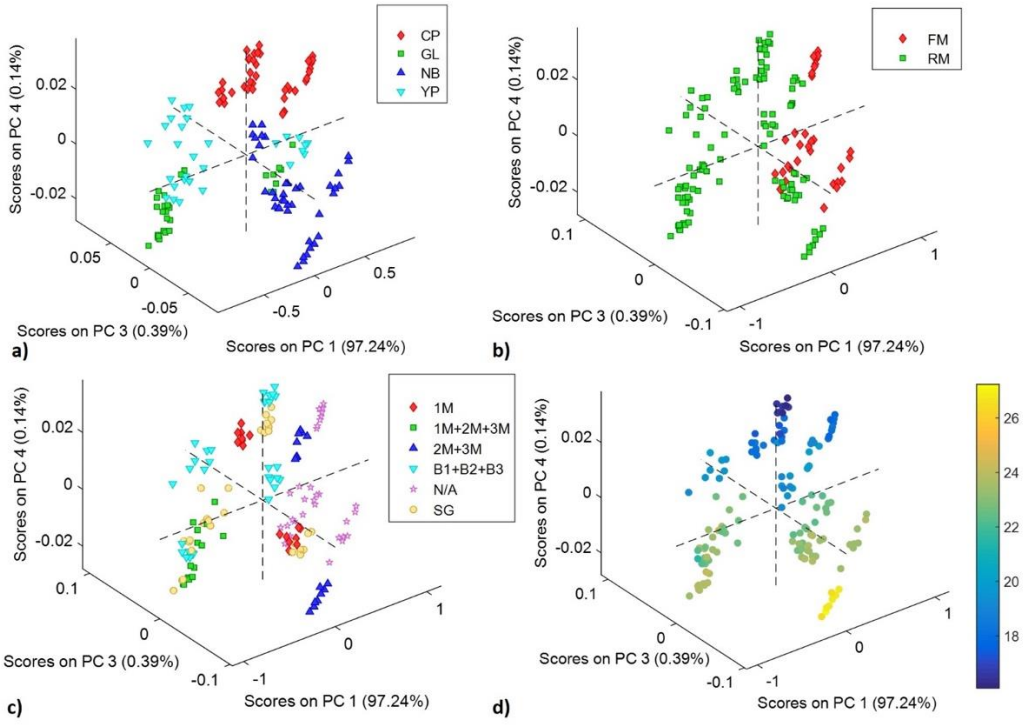

Figure 3.5 a) PC scores plot for PC1, PC3, and PC4 separated by pulse flour type b) PC scores plot for PC1, PC3 and PC4 separated by milling type c) PC scores plot for PC1, PC3 and PC4 separated by stream type d) PC scores plot for PC1, PC3, and PC4 separated by protein content

In the case of the pixel-based classification approach, a PCA model was developed by utilizing the pixels of the concatenated hyperspectral image from roller and Ferkar mills. The first two PCs explained major variance in the data where PC1 explained 90.54% of the total variance and PC2 explained 8.95% of the variance. Groupings based on the milling method were clearly depicted in PC2 since PC1 captured the noise in images. Figure 3.6a shows a PCA based classification map of the pulse flours based on milling method.

The wavelength band region of 1460 to 1600 nm contributed to the first overtone of N-H region (protein) with RNH_2 structure having a peak at 1530 nm. Similarly, the absorption band region of 1820 to 2000 nm can be attributed to the second overtone of C=O stretch and O-H combinations.

There are three peaks in 1860, 1900, and 1950 nm in this region. The peak at 1860 nm has C-C1 stretch with sixth overtone of C-C1 structure. The other peaks have C=O stretch with second overtone of CO_2-H (1900 nm) and CO_2-R (1950 nm) structures (Chen et al. 2013; Xiaobo et al. 2010). These chemical components can be attributed to the protein (N-H), fat (C=O), and moisture (O-H) content of the samples.

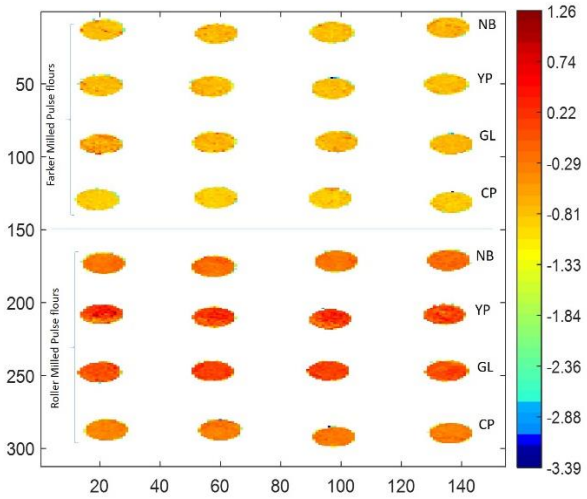

Figure 3.6 a) PC scores plot PC1 vs PC5 separated by milling method b) PC loadings plot for PC1

3.5.2 PLS-DA based supervised classification

3.5.2.1 Classification of pulse flours based on the pulse-type

In the case of the spectra-based classification of the mean-centered data, the PLS-DA model resulted in 5 latent variables (LVs) which accounted for 99.98% of the total covariance in the data. All four classes of pulse flours depicted 100% correct classification rate for both calibration and cross-validation (contiguous blocks with 9 data splits). The sensitivity and specificity values for each class in this case were recorded to be 1.00. Out of the 95 samples in the calibration dataset, 33 chickpea flours, 21 green lentil flours, 23 navy bean flours, and 18 yellow pea flours were correctly classified. The reliability of this calibration model was assessed by developing an external prediction model, the results of which yielded 100% classification accuracy. Thus, the error rate in the case of calibration, cross-validation, and the external prediction was zero. Table

3.1. depicts the confusion matrix for the spectra-based classification of flour samples based on pulse-type.

Table 3.1 Confusion matrix for pulse-type based classification (spectra-based)

Spectra-based classification								
Calibration		Actual class				N	Global	
		CP	GL	NB	YP		SENS	SPEC
Predicted as class	CP	33	0	0	0	33	1.00	1.00
	GL	0	21	0	0	21	1.00	1.00
	NB	0	0	23	0	23	1.00	1.00
	YP	0	0	0	18	18	1.00	1.00
	Total					95	Non-error rate: 100%	
Cross validation		Actual class				N	Global	
		CP	GL	NB	YP		SENS	SPEC
Predicted as class	CP	33	0	0	0	33	1.00	1.00
	GL	0	21	0	0	21	1.00	1.00
	NB	0	0	23	0	23	1.00	1.00
	YP	0	0	0	18	18	1.00	1.00
	Total					95	Non-error rate:	

								100%
External Prediction		Actual class				N	Global	
Predicted as class		CP	GL	NB	YP		SENS	SPEC
	CP	7	0	0	0	7	1.00	1.00
	GL	0	9	0	0	9	1.00	1.00
	NB	0	0	12	0	12	1.00	1.00
	YP	0	0	0	14	14	1.00	1.00
		Total				42	Non-error rate: 100%	

The regression vectors and the loadings plots for all the four types of pulse flours depicted sharp peaks in the region from 530 to 700 nm indicating that color played an important role in classification of flours. The navy bean, green lentil, and yellow pea flours were discriminated in the wavelength region from 540 to 700 nm. On the other hand, the chickpea flours were discriminated at 520, 540, and 670 nm, and possessed the highest weight in the PLS-DA model. The region from 530 nm to 560 nm can be attributed to the green band and 560 to 590 nm is related to the yellow band (Liang et al. 2020). Liang et al. (2020) found similar optimal wavelength peaks using the genetic algorithm (GA) to discriminate wheat flours. Therefore, this wavelength region possesses high credibility for the classification of flour samples based on color attributes.

For pixel-based classification, the PLS-DA model was developed on the mean-centered concatenated hyperspectral images with an overall non-error rate of 99% in calibration and 100% cross-validation. The confusion matrix for the pixel-based classification is shown in Table 3.2.

Table 3.2 Confusion matrix for pulse flour based classification (pixel-based)

Pixel-based classification								
Calibration		Actual class				Not assigned	Global	
		CP	GL	NB	YP		SENS	SPEC
Predicted as class	CP	4331	0	0	0	125	1.00	1.00
	GL	0	4305	21	3	180	0.99	1.00
	NB	0	54	4142	2	375	0.99	1.00
	YP	0	1	4	4258	232	1.00	1.00
							Non-error rate: 99%	
Cross validation		Actual class				Not assigned	Global	
		CP	GL	NB	YP		SENS	SPEC
Predicted as class	CP	4331	0	0	0	125	1.00	1.00

	GL	0	4304	21	2	182	0.99	1.00
	NB	0	54	4145	2	372	0.99	1.00
	YP	0	1	4	4255	235	1.00	1.00
							Non-error rate: 100%	

Figure 3.7 depicts the classification map for the prediction model on the concatenated hyperspectral image pixels based on pulse-type. The sensitivity and specificity values for the pixels in the map were found to be 1.00. It is noteworthy that due to over-saturation of images in a few regions of interest, a handful (can we provide here an approx. percentage) of pixels were excluded and not assigned to any class. The highest number of unassigned pixels were in navy bean (owing to its highly reflective shiny white surface), followed by yellow pea, green lentil, and chickpea flours. The classification accuracy was assessed using 100% non-error rate of the prediction model.

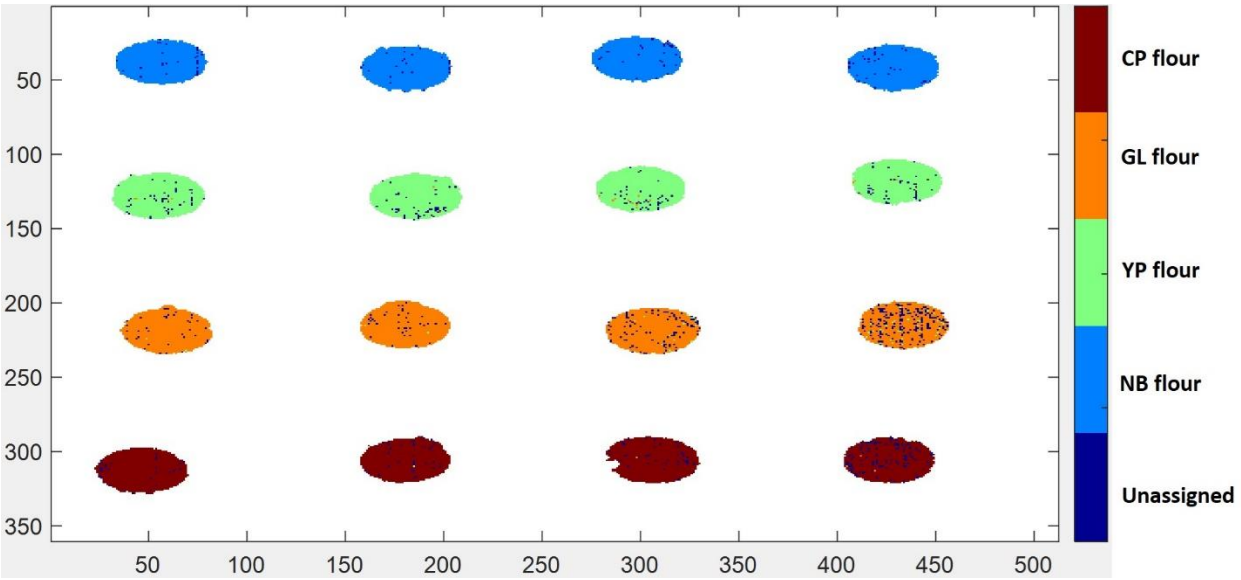

Figure 3.7 PLS-DA classification map for pulse-type based classification in the Vis-NIR range

3.5.2.2 Classification of pulse flours based on milling method

PLS-DA supervised classification models were developed in the SWIR range based on the satisfactory groupings observed in the PCA model. Various mathematical pre-treatments were applied, and first derivative followed by mean centering was found to be the most effective combination. The PLS-DA model comprised of two LVs with LV1 explaining 78.71% and LV2 explaining 11.56% of the total covariance in the data. The sensitivity and specificity values for both classes were 1.00, indicating 100% classification accuracy in calibration model. The cross-validation model developed using continuous blocks with nine data splits resulted in misclassification of one roller milled flour sample as Ferkar milled. Owing to this reason, the sensitivity of the roller mill sample dropped to 98.7% and the sensitivity of the Ferkar mill sample remained 100%. The wavelengths that contributed the most towards classification were found to be in the range of 1370 to 1500 nm, 1700 to 2000 nm, and 1900 to 1970 nm. The wavelength region of 1370 to 1500 nm is linked to water (O-H) and protein (N-H) bonds (Serranti, Cesare, and Bonifazi, 2013). This can be attributed to the higher protein content in roller mill streams when compared to Ferkar mill (no streams) (figure 3.5.d). The peaks in the region from 1900 to 1970 nm are due to O-H bending and stretching of water (Manley et al.

2011). Based on these observations, it can be concluded that milling method based classification in the SWIR range yields better results than Vis-NIR range because SWIR spectra captures the differences in chemical composition of samples. Table 3.3 shows the classification statistics of the PLS-DA model in calibration, cross validation, and external prediction.

Table 3.3 Confusion matrix for milling method based classification (spectra-based)

Spectra-based classification						
Calibration	Actual class			N	Global	
Predicted as class		FM	RM		SENS	SPEC
	FM	22	0	22	1.00	1.00
	RM	0	77	77	1.00	1.00
	Total			99	Non-error rate: 100%	
Cross validation	Actual class			N	Global	
Predicted as class		FM	RM		SENS	SPEC
	FM	22	1	22	1.00	0.99

	RM	0	76	77	0.99	1.00
	Total			99	Non-error rate: 99.5%	
External Prediction		Actual class		N	Global	
Predicted as class		FM	RM		SENS	SPEC
	FM	10	0	10	1.00	1.00
	RM	0	33	33	1.00	1.00
	Total			43	Non-error rate: 100%	

Additionally, PLS-DA classification models were developed based on the milling methods using the concatenated hyperspectral images. In this case, with first derivative followed by mean centering as a pre-treatment, the model yielded a classification accuracy of 95% in both calibration and cross-validation. For profound analysis of calibration model performance, sensitivity and specificity values were observed, which showed higher sensitivity for Ferkar mill (0.96) than roller mill (0.94).

Table 3.4 Confusion matrix for pulse flour mill based classification (pixel-based)

Pixel-based classification						
Calibration	Actual class			Not assigned	Global	
		FM	RM		SENS	SPEC
Predicted as class	FM	25	11	0	0.96	0.94
		30	0			
	RM	14	24	0	0.94	0.96
		7	41			
					Non-error rate: 95%	
Cross validation	Actual class			Not assigned	Global	
		FM	RM		SENS	SPEC
Predicted as class	FM	25	12	0	0.94	0.95
		16	4			
	RM	14	24	0	0.95	0.94
		8	40			
					Non-error rate: 94.5%	

From calibration and cross-validation models (Table 3.4), it can be observed that a higher number of pixels from Ferkar mill flour samples were misclassified as roller milled. However, none of the pixels in this classification models were unassigned. Figure 3.8 depicts the prediction map for the pulse flour samples classified as Ferkar milled, and roller milled. After finalizing the calibration model, the prediction map for milling method based classification was developed that yielded a prediction accuracy of 95%.

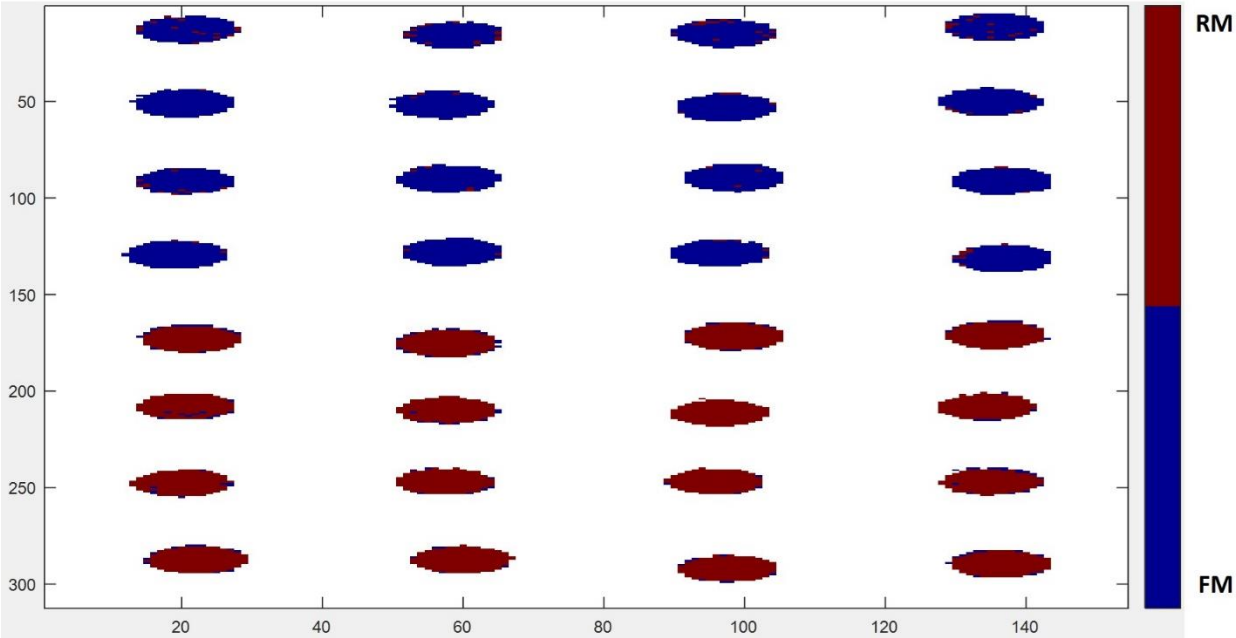

Figure 3.8 PLS-DA classification map for milling based classification in the SWIR range

3.6 Conclusion

This novel approach to explore the potential of a non-destructive and non-contact method for pulse flour classification has established that pulse-type can be classified using Vis-NIR range based on color attributes. Furthermore, green, and yellow bands played a significant role in classifying the flours based on pulse-type. Milling method, on the other hand is better captured in the SWIR spectra as it exploits the chemical composition (especially of the O-H and N-H overtones) of the samples. It can be concluded that both wavelength ranges contributed towards the classification goals, but the accuracies of milling method can be enhanced by enlarging the number of samples in the datasets. As for the two multivariate data techniques deployed,

supervised classification using PLS-DA yielded better results as compared to the unsupervised PCA analysis.

3.7 Acknowledgements

The authors acknowledge Agriculture and Agri-Food Canada's Canadian Pulse Science Research Cluster program and Natural Sciences and Engineering Research Council of Canada's Discovery Grants program for financial support. We also thank Canada Foundation for Innovation for infrastructural support We also thank Canada Foundation for Innovation for infrastructural support, Canadian International Grains Institute (Cigi) for their assistance in milling. A note of thanks is also due to Dr. Catherine Findlay for her help in writing of this manuscript.

References

Abdullah, M. M. H., C. P. F. Marinangeli, P. J. H. Jones, and J. G. Carlberg. 2017. Canadian potential healthcare and societal cost savings from consumption of pulses: A cost-of-illness analysis. *Nutrients* 9(7):1–22. https://doi.org/10.3390/nu9070793.

Ambrose, A., and B.K. Cho. 2014. A Review of Technologies for Detection and Measurement of Adulterants in Cereals and Cereal Products. *Journal of Biosystems Engineering* 39(4): 357–365. https://doi.org/10.5307/jbe.2014.39.4.357.

Babellahi, F., J. Paliwal, C. Erkinbaev, M. L. Amodio, M. M. A. Chaudhry, and G. Colelli. 2020. Early detection of chilling injury in green bell peppers by hyperspectral imaging and chemometrics. *Postharvest Biology and Technology* 162(September 2019) 111100. https://doi.org/10.1016/j.postharvbio.2019.111100.

Castorena, J., J.Morrison, J. Paliwal, and C. Erkinbaev. 2015. Non-uniform system response detection for hyperspectral imaging systems. *Infrared Physics and Technology* 73:263–268. https://doi.org/10.1016/j.infrared.2015.10.002.

Chaudhry, M. M. A., M. L. Amodio, F. Babellahi, M. L. V. de Chiara, J. M. Amigo Rubio, and G.Colelli. 2018. Hyperspectral imaging and multivariate accelerated shelf life testing (MASLT) approach for determining shelf life of rocket leaves. *Journal of Food Engineering* 238(June):122–133. https://doi.org/10.1016/j.jfoodeng.2018.06.017.

Chen, J., X. Ren, Q. Zhang, X. Diao, and Q. Shen. 2013. Determination of protein, total carbohydrates and crude fat contents of foxtail millet using effective wavelengths in NIR spectroscopy. *Journal of Cereal Science* 58(2):241–247. https://doi.org/10.1016/j.jcs.2013.07.002.

ElMasry, G., M. Kamruzzaman, D. W. Sun, and P. Allen. 2012. Principles and Applications of Hyperspectral Imaging in Quality Evaluation of Agro-Food Products: A Review. *Critical Reviews in Food Science and Nutrition* 52(11):999–1023. https://doi.org/10.1080/10408398.2010.543495.

Erkinbaev, C., K. Derksen, and J. Paliwal. 2019. Single kernel wheat hardness estimation using near infrared hyperspectral imaging. *Infrared Physics and Technology* 98(March):250–255. https://doi.org/10.1016/j.infrared.2019.03.033.

Guillermic, R. M., E. C. Aksoy, S. Aritan, C. Erkinbaev, J. Paliwal, and F. Koksel. 2021. X-Ray microtomography imaging of red lentil puffed snacks: Processing conditions, microstructure and texture. *Food Research International* 140:109996. https://doi.org/10.1016/j.foodres.2020.109996.

Liang, K., J. Huang, R.He, Q. Wang, Y. Chai, and M. Shen. 2020. Comparison of Vis-NIR and SWIR hyperspectral imaging for the non-destructive detection of DON levels in Fusarium head blight wheat kernels and wheat flour. *Infrared Physics and Technology* 106(40): 103281. https://doi.org/10.1016/j.infrared.2020.103281.

Luo, S., E. Chan, M. T. Masatcioglu, C. Erkinbaev, J. Paliwal, and F. Koksel. 2020. Effects of extrusion conditions and nitrogen injection on physical, mechanical, and microstructural properties of red lentil puffed snacks. *Food and Bioproducts Processing* 121:143–153. https://doi.org/10.1016/j.fbp.2020.02.002.

Manley, M., G. Du Toit, and P. Geladi. 2011. Tracking diffusion of conditioning water in single wheat kernels of different hardnesses by near infrared hyperspectral imaging. *Analytica Chimica Acta* 686:64–75. https://doi.org/10.1016/j.aca.2010.11.042.

Maskus, H., L. Bourré, S. Fraser, A. Sarkar, and L. Malcolmson. 2016. Effects of grinding method on the compositional, physical, and functional properties of whole and split yellow pea flours. *Cereal Foods World* 61(2):59–64. https://doi.org/10.1094/CFW-61-2-0059.

Mishra, P., A. Herrero-Langreo, P. Barreiro, J. M. Roger, B. Diezma, N. Gorretta, and Lleó, L. 2015. Detection and quantification of peanut traces in wheat flour by near infrared hyperspectral imaging spectroscopy using principal-component analysis. *Journal of Near Infrared Spectroscopy* 23(1):15–22. https://doi.org/10.1255/jnirs.1141.

Mobaraki, N., and Amigo, J. M. (2018). HYPER-Tools. A graphical user-friendly interface for

hyperspectral image analysis. *Chemometrics and Intelligent Laboratory Systems*, *172*(November 2017):174–187. https://doi.org/10.1016/j.chemolab.2017.11.003.

Schutyser, M. A. I., P. J. M. Pelgrom, A. J. van der Goot, and R. M. Boom. 2015. Dry fractionation for sustainable production of functional legume protein concentrates. *Trends in Food Science and Technology* 45(2):327–335. https://doi.org/10.1016/j.tifs.2015.04.013.

Serranti, S., D. Cesare, and G. Bonifazi. 2013. The development of a hyperspectral imaging method for the detection of Fusarium-damaged, yellow berry and vitreous Italian durum wheat kernels. *Biosystems Engineering* 115(1):20–30. https://doi.org/10.1016/j.biosystemseng.2013.01.011.

Su, W. H., and D. W. Sun. 2018. Fourier Transform Infrared and Raman and Hyperspectral Imaging Techniques for Quality Determinations of Powdery Foods: A Review. *Comprehensive Reviews in Food Science and Food Safety* 17(1):104–122. https://doi.org/10.1111/1541-4337.12314.

Thakur, S., M. G. Scanlon, R. T. Tyler, A. Milani, and J. Paliwal. 2019. Pulse Flour Characteristics from a Wheat Flour Miller's Perspective: A Comprehensive Review. *Comprehensive Reviews in Food Science and Food Safety* 18(3):775–797. https://doi.org/10.1111/1541-4337.12413.

Xiaobo, Z., Z. Jiewen, M. J. W. Povey, M. Holmes, and Hanpin, M. 2010. Variables selection methods in near-infrared spectroscopy. *Analytica Chimica Acta* 667(1–2):14–32. https://doi.org/10.1016/j.aca.2010.03.048.

CHAPTER 4. Pulse flours characterization using scanning electron microscopy

This chapter is based on the manuscript submitted in the journal Food and Bioprocess technology entitled ‘Pulse flours characterization using scanning electron microscopy’.

4.1 Abstract

Increasing consumer interest in pulse flour-based food formulations has highlighted the importance of flour characterization based on pulse type and milling method. The present study aimed to compare the microstructure of four different pulse flours (chickpea, navy bean, green lentil, and yellow pea) obtained from two milling methods (single-stage Ferkar mill and multi-stage roller mill). Scanning electron microscopy was used to explore the relationship between particle size distribution and protein content, along with the characterization of starch-protein matrices. Micrographs depicted that protein bodies were finely distributed in Ferkar-milled flours and straight grade stream of roller-milled flours with similar protein content. The reduction flour stream (possessing the highest protein content) contained more damaged starches than the break flour stream (possessing the lowest protein content). The presence of pores was higher in chickpea starches as compared to the other pulse flours. Navy bean flours possessed the highest starch protein cluster count. Traces of bran particles were clearly visible in green lentil flours obtained from roller and Ferkar mills. Conclusively, the microstructure and protein content of the pulse flours is influenced by the pulse type and milling method.

Keywords: pulse, milling, protein, particle size, micrographs

4.2 Introduction

Plant-based diets are being preferred by the health-conscious consumers who have increased awareness of the impact of agricultural practices on the environment (Carlsson-Kanyama and González 2009; Röös et al. 2017). Pulses are well suited to serve this market due to their high protein content and nutritional density (Diaz-contreras et al. 2021). Despite limiting concentrations of sulfur-containing amino acids, pulses are a rich source of lysine that, when sufficiently combined with cereals, establishes a complete amino acid profile necessary for a healthy diet (Young and Pellett 1994). It is noted that regular consumption of pulses in whole or processed form improves gut health and reduces the risk of cardio-vascular diseases, cancer, and diabetes (Abdullah et al., 2017). Pulse crops are also important to include into cyclic crop rotations for the facilitation of sustainable food chains. Being drought-resistant crops, pulse crops improve soil fertility by converting atmospheric nitrogen into nitrogen compounds with the help of symbiotic bacteria *(Rhizobium and Bradyrhizobium)* (Hossain et al. 2016) and contribute to the diversity of soil microbe communities. Researchers have developed bread, cookies, tortillas, pasta, noodles, puffed snacks using pulse flours such as chickpea, navy bean, green lentil, and yellow pea (Anton et al. 2008; Han et al., 2010; Maskus et al., 2016; Osorio-Diaz et al. 2008).

Studies have shown pulse flour composition and particle size influence the end-quality of food products (Bourré et al., 2019; Maskus et al., 2016; Young et al., 2020). In the modern food industry, adequate knowledge of pulse flour properties is a prerequisite to mitigate variability and supply quality products at retail. Pulse milling technology and its applied settings directly affect flour physicochemical properties such as the particle size distribution, protein quality and starch damage (Scanlon et al., 2018). These properties will consequently influence flour hydration and dough structure and, as a result, sensory characteristics such as texture, crunchiness, crispiness, and consumer acceptability may vary. Very few research works have characterized starch-protein matrices while exploring the relationship between particle size distribution and protein content of pulse flours from different milling methods. For instance, flours milled using a hammer mill, pin mill, roller mill, and stone mill depicted differences in their protein contents (Maskus et al., 2016; Schutyser et al., 2015; Thakur et al., 2019) but the

actual microstructural changes consequential to different milling methods of pulses have yet to be explored.

Various imaging techniques such as optical microscopy, X-ray microtomography, magnetic resonance imaging, atomic force microscopy, confocal fluorescence microscopy, and scanning electron microscopy (SEM) have been used to investigate the microstructure of whole pulse and flour samples (Aguilera 2005; Ramachandran et al. 2021). SEM has successfully been utilized by a number of studies as a suitable method for investigating starch-protein matrices in flours (Assatory et al. 2019; Pelgrom et al. 2015b; Schutyser et al. 2015). The advantage of SEM over other techniques is that it provides higher magnifications (20 to 10,000×) which assists in efficiently exploring the particle size and component separation in flour samples (Aguilera and Germain 2007). Cloutt et al. (1987) stated the significance of starch granule size in the separation of starch-protein matrix during air classification of pulse flours. Similarly, (Pelgrom et al. 2015a) reported that larger starch granules were more likely to enter the fine fraction that lowers the protein content of chickpea flours. Li et al. (2019) used SEM to compare the starches from pea, lentil, and faba bean with commercial starches. The study concluded that the starches obtained from air-classified flours possessed broken granules and starches whereas the commercial pea starch obtained from wet extraction showed no such features. The damaged starch granules from the lentil starches were similar to those obtained from the commercial pea starches.

The aim of this research work is to utilize SEM for the investigation of differences in the microstructures of four pulse flours (chickpea, navy bean, green lentil, and yellow pea) obtained from two milling methods (single-stage Ferkar mill and multi-stage roller mill). Particle size distribution, protein content and characteristics of starch-protein matrices of flours based on pulse type and milling method were investigated.

4.3 Materials and Methods

4.3.1 Raw materials and milling

Green lentils (CDC Greenstar), chickpeas (CDC Orion), and yellow peas (CDC Spectrum) were acquired from Reisner farm in Limerick, Saskatchewan, and navy beans (Nautica) were obtained from Hensall Co-op in Hensall, Ontario (2018 growing season). The moisture and protein

contents of the whole chickpea, navy bean, green lentil, and yellow pea were measured as 12.2%, 13.3%, 9.9%, and 12.4% (wet basis) and 20.0%, 25.7%, 24.9%, and 23.7% (dry basis), respectively. Milling of the whole pulses was done at the Canadian International Grains Institute (Cigi), Winnipeg. Prior to milling, pulses were treated to a pre-break step using Jacobson hammer mill (Model 120-B, Jacobson Inc., Iowa, U.S.) with 3.175 mm screen. For the roller mill and Ferkar mill, 5 kg and 3 kg of each whole pulse were used, respectively. A single-stage, Ferkar multi-purpose knife mill (model: Ferkar 5; KFM, Slovenia) with a 140 µm screen, 50 Hz motor and 8 Hz feed rate was used. The lab roller mill (Buhler, MLU 202 laboratory mill; Buhler Group, Switzerland) is comprised of break and reduction systems. The three break rolls were set at B1 (0.1 mm), B2 (0.01 mm), and B3 (0.01 mm) with a screen size of 475 µm/132 µm for B1 and B2 rolls, and 375/132 µm for B3 rolls. The three reduction rolls (1M, 2M, 3M) had a clearance of 0.01 mm with a screen size of 150 µm /150 µm. The number of roller mill replicates was 28 whereas 8 replicates were obtained from Ferkar mill.

4.3.2 Stream blends (roller mill)

Stream blends were formulated by combining flours produced from six streams (B1, B2, B3, 1M, 2M, 3M) of roller mill. Break flour stream (B1+B2+B3) was a combination of flours from B1, B2, and B3 streams for all the pulse types. The reduction flour or middling flour stream (1M+2M+3M) was formulated by combining flours from 1M, 2M, and 3M streams for green lentil and yellow pea flours. In case of chickpea and navy bean flours, two separate reduction flours were made, based on yield. The first flour stream comprised of 1M flour stream (1M) and second stream was a combination of 2M and 3M flour streams (2M+3M). All six flour streams were blended to produce straight grade (SG) flours stream that was proportional to the total yield of the milled product. The flour yield for each pulse-type and streams for roller mill is given in Table 4.1

Table 4.1 Flour yield of roller mill streams

% Yield (total products basis)

	Green Lentil		Yellow Pea		Chickpea		Navy Bean	
Stream	Replicat	Replicat	Replicat	Replicat	Replicat	Replicat	Replicat	Replicat

	e A	e B	e A	e B	e A	e B	e A	e B
B1	6.2	6.0	7.3	8.0	11.9	11.8	7.8	7.6
B2	6.5	6.8	6.8	7.2	7.2	7.1	7.2	7.0
B3	3.3	2.9	3.3	3.2	2.8	3.4	4.1	5.0
1M	70.6	69.3	68.1	68.4	51.1	51.6	45.7	44.2
2M	4.2	5.9	5.8	4.8	16.6	15.9	20.9	21.5
3M	0.7	0.8	1.0	0.8	4.8	4.5	5.6	5.9
Shorts	2.3	2.6	0.7	0.5	1.2	1.1	1.4	1.3
Hulls	6.2	5.8	7.0	7.1	4.4	4.5	7.4	7.5
Straight Grade	91.5	91.6	92.3	92.4	94.4	94.4	91.3	91.2

4.3.3 Scanning electron microscopy

The scanning electron microscope (SEM) (Quanta 650 FEG ESEM, FEI Company, USA) was utilized with an accelerating voltage of 5kV. The samples were sputter coated (20 nm/min for 45 s) with gold-palladium in a sputter coater (Desk II Denton Vacuum, LLC, USA) and photographed at five different magnifications (50, 200, 1000, 2500, and 5000×). A total of 36 samples were studied including the milling replicates. SEM imaging was done in duplicate for each milling replicate formulating an imaging dataset of 72 samples in total. Particle sizes were measured using FEI xT microscope control software. The average particle size of milled pulse flours was calculated by taking the average diameter (longest length) of 200 particles.

4.3.4 Protein content

LECO FP-628 (LECO Corp., USA) was used for the protein content determination following the method proposed by Williams et al. (1998). The conversion factor, N×6.25 was used to calculate the protein values where N represents the nitrogen content. Daily drift corrections were done using Ethylenediaminetetraacetic acid (EDTA). The protein content was determined in duplicate for each of the 72 samples to account for the variance in the data.

4.3.5 Statistical analysis

R-Studio (Version 1.3.1093, PBC, USA) software was used to plot particle size distribution using the density plot function. Furthermore, SPSS (Version 22, IBM, Statistics Corp., USA) software was used to calculate descriptive statistics measures (such as average, median, interquartile range, range, and standard deviation), as well as to perform analysis of variance (ANOVA). Particle size dimension and protein content were analyzed using one-way classic ANOVA. In this case, the differences between means were evaluated using Tukey-Kramer test ($p<0.05$). Welch ANOVA with Games-Howell post hoc test was used for samples that failed the variances test homogeneity ($p<0.05$). It was observed that both Welch ANOVA and classic ANOVA reported equivalent results. Stream-based and pulse type classifications were carried out to study the relationship between particle size distribution, protein content, and characteristics of starch-protein matrix of the pulse flours.

4.4 Results and discussions

4.4.1 Particle size distribution

The boxplot in Figure 4.1 depicts the particle size distribution of all milled pulse flours. Variability across samples suggest that pulse type and milling streams may cause significant changes in terms of particle size distributions. The particles were found to be in the range of 5-51 µm with cellular fragments and protein bodies below 5 µm. These results are in agreement with other studies; Pelgrom et al. (2015b) determined impact milled pre-treated whole pea flour particles in the range of 22-26 µm to be associated with starch granules and 1-10 µm with protein bodies and parts of cell wall, respectively. Another study evaluating the impact of milled whole pulses (beans, peas and lentils) in which the particle size distribution of beans and lentils showed a distinctive peak (around 4-5 µm) attributed to protein bodies as compared to chickpeas because the starch granules of chickpeas had similar sizes as those of protein bodies thus decreasing separation sharpness Pelgrom et al.(2015a). The authors also stated that the size of protein bodies is larger in beans than peas (Pernollet 1978), indicating differences among pulse types for protein body and starch granule sizing in the respective flours. By using SEM imaging, Pelgrom et al. (2013) confirmed with SEM imaging that in case of impact/jet milled whole pea flours, particle sizes of 1-3 µm represent protein bodies whereas starches possess a particle size of 22 µm and particles above 40 µm can be categorized as whole cells or parts of cells. The

particle distribution in Figure 4.1 can therefore be attributed to protein bodies (1-5 µm), starch granules (15-40 µm), and the whole or parts of the cells (above 40 µm), although differences across pulse types may occur.

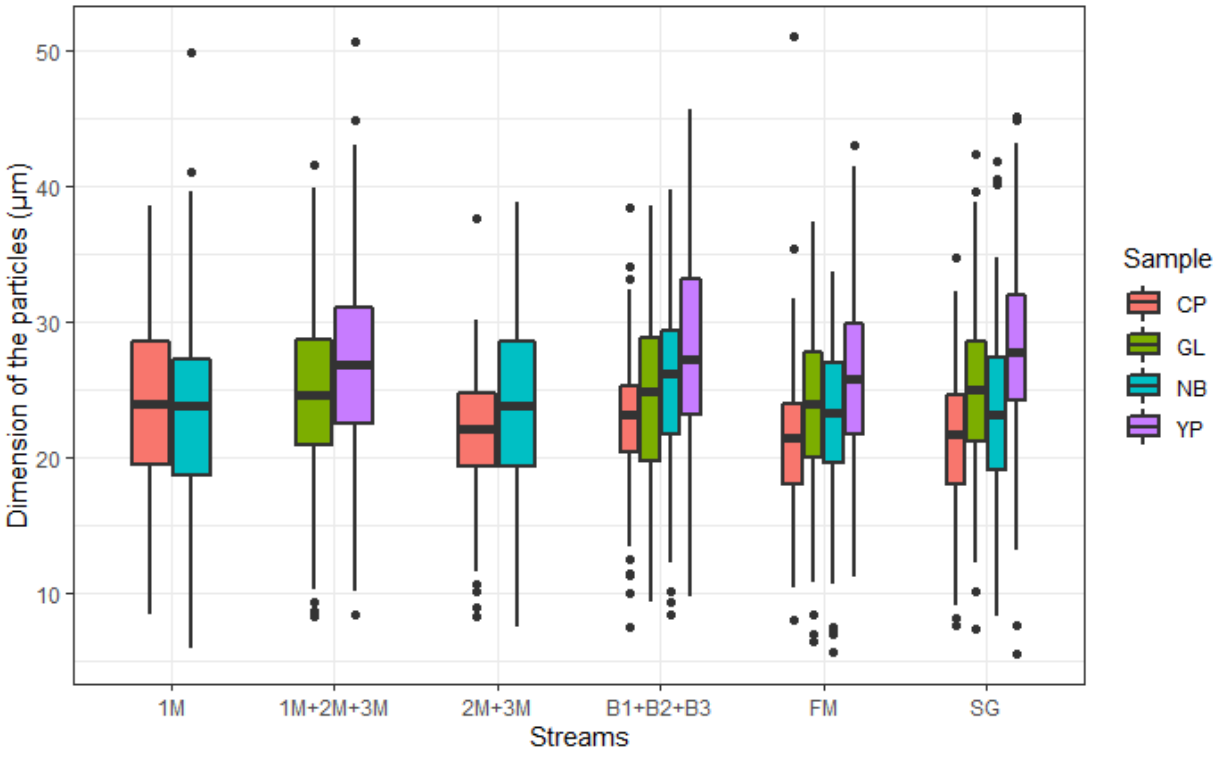

Figure 4.1. Particle size distribution of the different pulse flours milled using Ferkar mill and roller mill. FM- Ferkar mill (one stream); Roller mill streams – SG, B1+B2+B3,1M+2M+3M, 1M, 2M+3M; CP-chickpeas, GL- green lentils, NB- navy beans, YP- yellow peas

4.4.1.1 Particle size distribution across mill streams

Density curve plots of flour derived from Ferkar and roller milled pulse flours are presented in Figure 4.2. Some differences were noted among Ferkar mill and roller mill SG streams (Figure 4.2a and 4.2b) including a narrower distribution for Ferkar mill flours as demonstrated by a smaller interquartile region (IQR) compared to roller mill SG streams, 5.92-8.20 µm vs. 6.51-8.55 µm, respectively, across pulse types. This could be attributed to the various forces of action

of the Ferkar mill (cutting and shearing forces) relative to roller mill (compression, shear, and frictional forces) resulting in differentially fractured seeds and thus distinct particle size and density characteristics of the resulting flour (Thakur et al. 2019). Roller mill B1+B2+B3 streams skewed slightly right relative to other flour streams, showing greater number of particles distributed (based on IQR) in the range of 20-35 µm for navy bean and green lentil flours, and 20-32 µm in case of yellow pea flours (Figure 4.2c).The highest average particle size of milled pulse flours was found to be in yellow pea flours in both the mills for all streams (FM- 25.80 ± 5.86 µm, SG- 28.19 ± 6.55 µm, 1M+2M+3M- 26.84 ± 6.78 µm) except for green lentil flours in B1+B2+B3 (27.83 ± 6.67 µm) stream. Navy bean depicted higher average particle size for 1M (23.31 ± 6.73 µm) and 2M+3M (23.92 ± 6.41 µm) streams relative to chickpea flour (see Table 4.2).

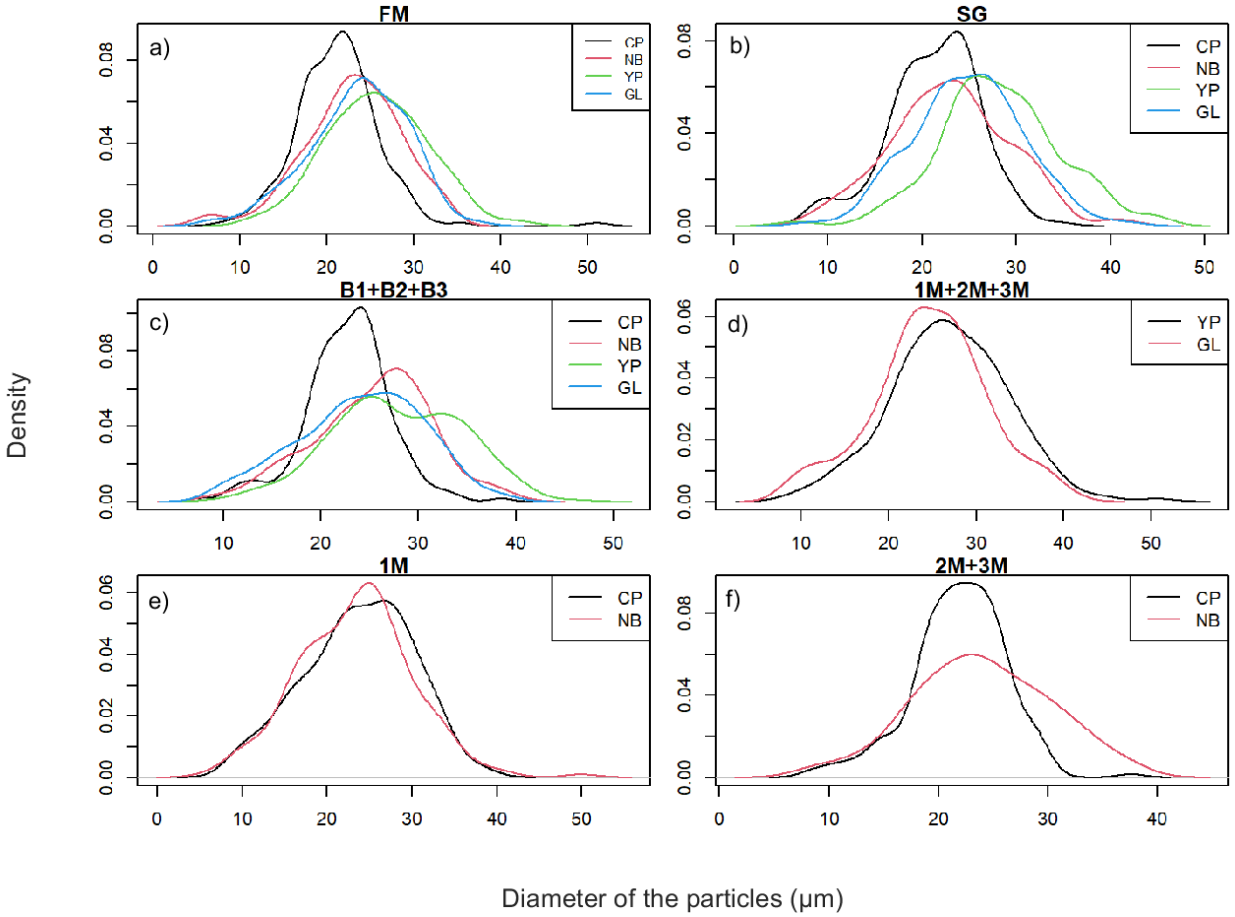

Figure 4.2 Density plot across flour streams derived from a) Ferkar mill (FM) b) Straight grade (SG) c) Break stream (B1+B2+B3) d) Reduction stream (1M+2M+3M) e) Reduction stream (chick peas and navy beans) (1M) f) Reduction stream (chick peas and navy beans) (2M+3M)

Table 4.2 shows ANOVA results for particle size distribution and protein content as analyzed across mill streams and pulse types. Flours derived from peas, lentils, chickpeas, and navy beans differed significantly ($p < 0.05$) in average particle size and protein content across mill streams with the exception of average particle size for navy bean and chickpea 1M roller mill flour streams. This result is indicative of a crop specific influence on the properties of similarly milled pulse flours that may be attributed to the varying initial concentrations moisture and protein content in the whole pulse samples. Thakur et al. (2019) reported that attributes such as protein, seed toughness, fiber, lipid content, and cell wall thickness in the cotyledons have profound effect on milling performance. Additionally, the millability of each pulse may be affected by the strength of the bond between the hull and cotyledon which differs according to pulse type, where the flexible hull has different milling properties in comparison with brittle cotyledons (Bourré et al. 2019).

Table 4.2. Particle size distribution and protein content of Ferkar and roller milled flours as reported across mill streams and pulse types

Mill streams					**Pulse-type**				
Mill	**Streams**	**Sample**	**Average particle size (µm)**	**% Protein content**	**Sample**	**Mill**	**Stream**	**Average particle size (µm)**	**% Protein content**
FM	N/A	CP	21.23 ± 4.87 a	17.97±0.25 a	CP	FM	N/A	21.23 ± 4.87 a	17.97±0.25 a
		NB	22.99 ± 5.64 b, e	23.3 ±0.20 b		RM	SG	21.19 ± 4.87 a	18.05±0.70 a
		YP	25.80 ± 5.86 c	22.36±0.21 b			B1+B2+B3	22.67 ± 4.44 b, c, d	16.47±0.17 b
		GL	23.58 ± 5.65 d, e	22.52±0.18 c			1M	23.72 ± 6.40 c	18.07±0.31 a
RM	SG	CP	21.19 ± 4.87 a	18.05±0.70 a			2M+3M	21.87± 4.29 a, d	19.68±0.44 c
		NB	22.96 ± 6.37 b	23.49±0.12 b	NB	FM	N/A	22.99 ± 5.64 a	23.30±0.20 a
		YP	28.19 ± 6.55 c	22.57±0.14 a		RM	SG	22.96 ± 6.37 a	23.49±0.12 a
		GL	24.85 ± 5.86 d	23.65±0.17 c			B1+B2+B3	25.31 ± 6.08 b, c	19.40±0.34 b
	B1+B2+B3	CP	22.67 ± 4.44 a, d	16.47±0.17 a			1M	23.31 ± 6.73 a	23.40±0.16 c
		NB	25.31 ± 6.08 b, d	19.40±0.34 b			2M+3M	23.92 ± 6.41 a, c	26.66±0.26 a
		YP	24.06 ± 6.40 c	19.64±0.19 b	YP	FM	N/A	25.80 ± 5.86 a	22.36±0.21 a
		GL	27.83 ± 6.67 d	22.27±0.32 c		RM	SG	28.19 ± 6.55 b, d	22.57±0.14 a
	1M+2M+3M	YP	26.84 ± 6.78 *	23.03±0.36 *			B1+B2+B3	24.06 ± 6.40 c, d	19.64±0.19 b
		GL	24.65 ± 6.67 *	23.78±0.10 *			1M+2M+3M	26.84 ± 6.78 a, d	23.03±0.36 c
	1M	CP	23.72 ± 6.40	18.07±0.31 *	GL	FM	N/A	23.58 ± 5.65	22.52±0.18 a
		NB	23.31 ± 6.73	23.4 ± 0.16 *		RM	SG	24.85 ± 5.86	23.65±0.17 b
	2M+3M	CP	21.87± 4.29 *	19.68±0.44 *			B1+B2+B3	27.83 ± 6.67	22.27±0.32 a
		NB	23.92 ± 6.41 *	26.66±0.26 *			1M+2M+3M	24.65 ± 6.67	23.78±0.10 b

FM- Ferkar mill, RM- roller mill, CP-chickpeas, NB- navy beans, YP- yellow peas, GL- green lentils, N/A- not applicable

a Mean and standard deviation of replicate results of particle size distribution and % protein content of different pulse flours; Mean ± SD with a different letter in a column within the same pulse type and same stream are significantly different ($p < 0.05$), except for the stream (1M) and pulse (GL) in case of particle size distribution. * Samples are significantly different ($p < 0.05$); post-hoc test is not needed as only 2 groups were compared.

4.4.1.2 Particle size distribution across pulse-types

Figure 4.3. shows the density plot for pulse-type classifications of flours with various streams.

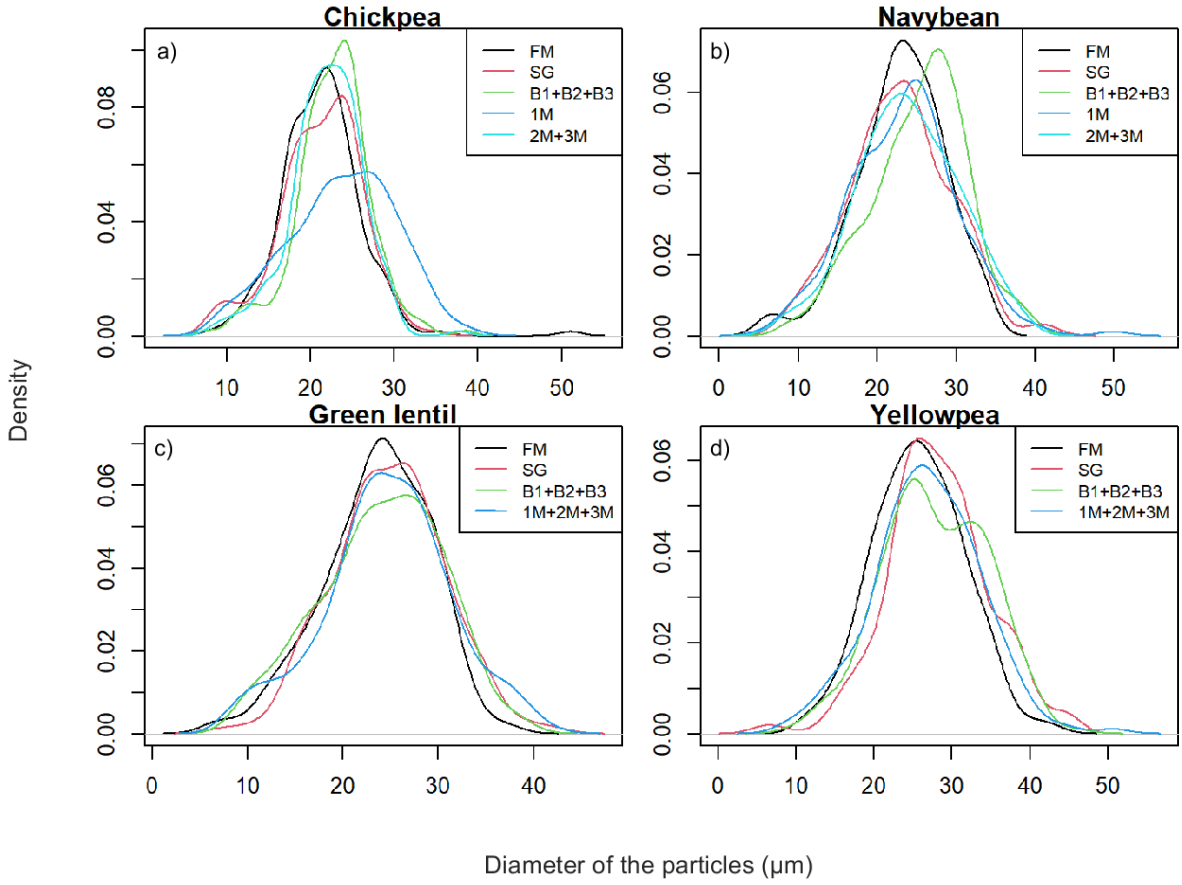

Figure 4.3. Density plot for pulse-type classification of flours a) Chickpea b) Navy bean c) Green lentil d) Yellow pea

A wide variation (based on IQR) in particle size distribution for green lentil, yellow pea and navy bean flours were observed in both the mills for all streams (Figure 4.3). For chickpea flours, the majority of particles were distributed between 18 and 27 µm (based on IQR) except for the roller mill stream 2M+3M where majority of the particles were distributed in 20-35 µm range. For all other pulse types, the average particle size of reduction streams was lower than those reported in break (B1+B2+B3) streams, although this difference was not statically significant (Table 4.2). For all lentil flours, the average particle size did not significantly differ

among mill streams, where significant differences were noted for all other pulse types (Table 4.2). The yield of flour streams varies due to particle size and density differences of the pulse flours.

4.4.2 Protein content

The protein contents of the whole chickpea, navy bean, green lentil, and yellow pea were measured as 20.0%, 25.7%, 24.9%, and 23.7% (average value in dry basis), respectively prior to milling. From Table 4.2, it can be found that the protein content of milled pulse flours was affected by the applied milling conditions, with differing degrees of variability within chickpea (21.3-23.7%), navy bean (23.0-25.3%), yellow pea (24.0-28.2%) and green lentil (23.6%-27.8%) flours.

4.4.2.1 Protein content across pulse- type

Table 4.2 presents the protein content of flours across mill streams. In all instances, chickpea flours displayed significantly lower protein content than remaining pulse types which is not surprising given whole chickpea seeds displayed the lowest initial protein levels. Protein content of lentil flours was significantly higher than other pulse types across mill streams (Table 4.2); this included navy bean which contained higher whole seed concentrations of protein prior to milling (24.9% vs 25.7%, respectively). This may be attributed to the ease of hull and cotyledon separation in the case of lentils, where this separation is considerably more difficult for beans (Thakur et al. 2019). Insufficient separation of the hull could explain the decrease in flour protein concentrations where parts of the cotyledon are removed as part of the hull fraction. In this study, a higher percentage of hulls were collected during the milling of navy beans (7.4-7.5%) relative to green lentils (5.8-6.2%; Table 4.1).

4.4.2.2 Protein content across mill streams

Table 2 presents the protein contents for Ferkar and roller according to pulse type. With the exception of lentil flour, there were no significant differences in the protein content between Ferkar milled and roller mill SG flours. However, results did indicate a significant difference according to the individual roller mill streams analyzed (Table 4.2). For all flours, protein levels

were significantly increased in reduction streams (1M+2M+3M, 1M, and 2M+3M) relative to break (B1+B2+B3) streams. In the case of chickpea and pea flours, the protein content of reduction streams was significantly higher than roller mill straight grade and Ferkar milled flours. Other studies have similarly reported higher protein concentrations in pulse flours derived from the reduction side of the mill; where protein content was found to be inversely related to particle size (Motte et al. 2021; Pelgrom et al. 2013; Sakhare et al. 2014; Thakur et al. 2019; Tyler 1984). During dry fractionation of legumes, Pelgrom et al. (2015a) reported lower protein content in chickpea flour as an increased number of larger particles entered the fine fraction. Sakhare et al. (2014) observed higher flour yield and protein content in reduction streams of roller-milled mung bean flours, attributed to more of the finer, protein-rich cotyledon particles from the break rolls being released by the sifter and further ground by the reduction rolls. In this study, ~70-75% of total flour yield was collected from 1M, 2M and 3M streams (Table 4.1). The significant differences in protein content across mill streams may be practically relevant for blending in which flours could be strategically tailored for specific end-use applications (Motte et al. 2021).

4.4.3 Characteristics of starch-protein matrix

4.4.3.1 SEM imaging of pulse flours across streams

Pulse starches were found to be oval, globular, round, or spherical in shape, with smooth surfaces.

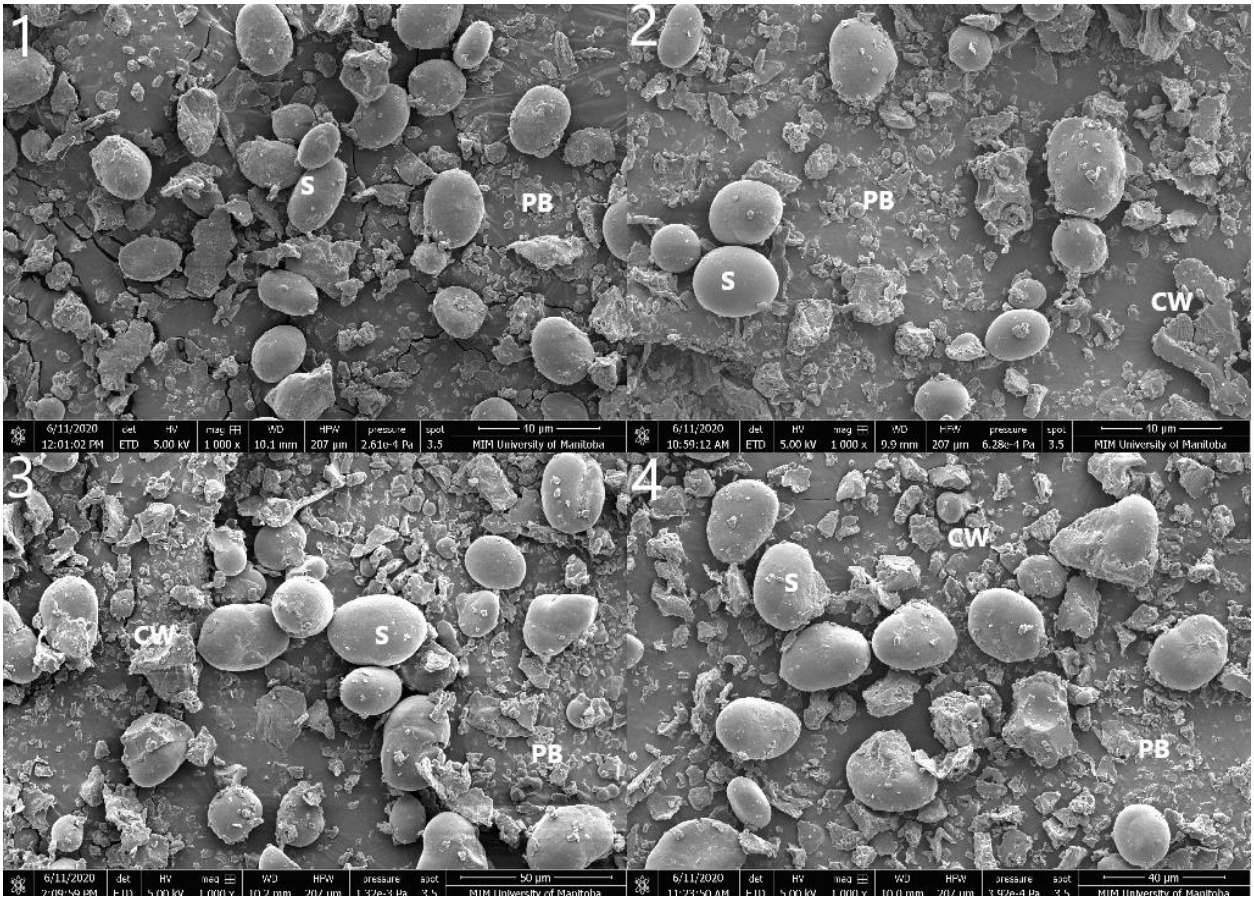

Figure 4.4. SEM images of Ferkar-milled samples (1000 × 1) Chickpeas 2) Navy beans 3) Green lentils 4) Yellow peas S-Starch, PB- Protein bodies, CW- Cell wall

Figure 4.4 shows the micrographs of Ferkar-milled pulse flours. The average particle size of the chickpea flour was 21.23±4.87 µm (Table 4.2). Whereas navy bean, green lentil, and yellow pea flours displayed average particle size of 22.99±5.64, 23.58±5.65, and 25.80±5.86 µm, respectively. It can be deduced that chickpea flours possess the lowest particle size in Ferkar-milled flours. Figure 4.5 demonstrates the microstructure of the SG roller-milled flours. The average particle size of chickpea, navy bean, green lentil and yellow pea flours were 21.19±4.87, 22.96±6.37, 24.85±5.86 and 28.19±6.55 µm, respectively. The particle size and protein contents of Ferkar and SG mill streams were found to be similar, with the exception of average particle size for yellow pea flours (Table 4.2).

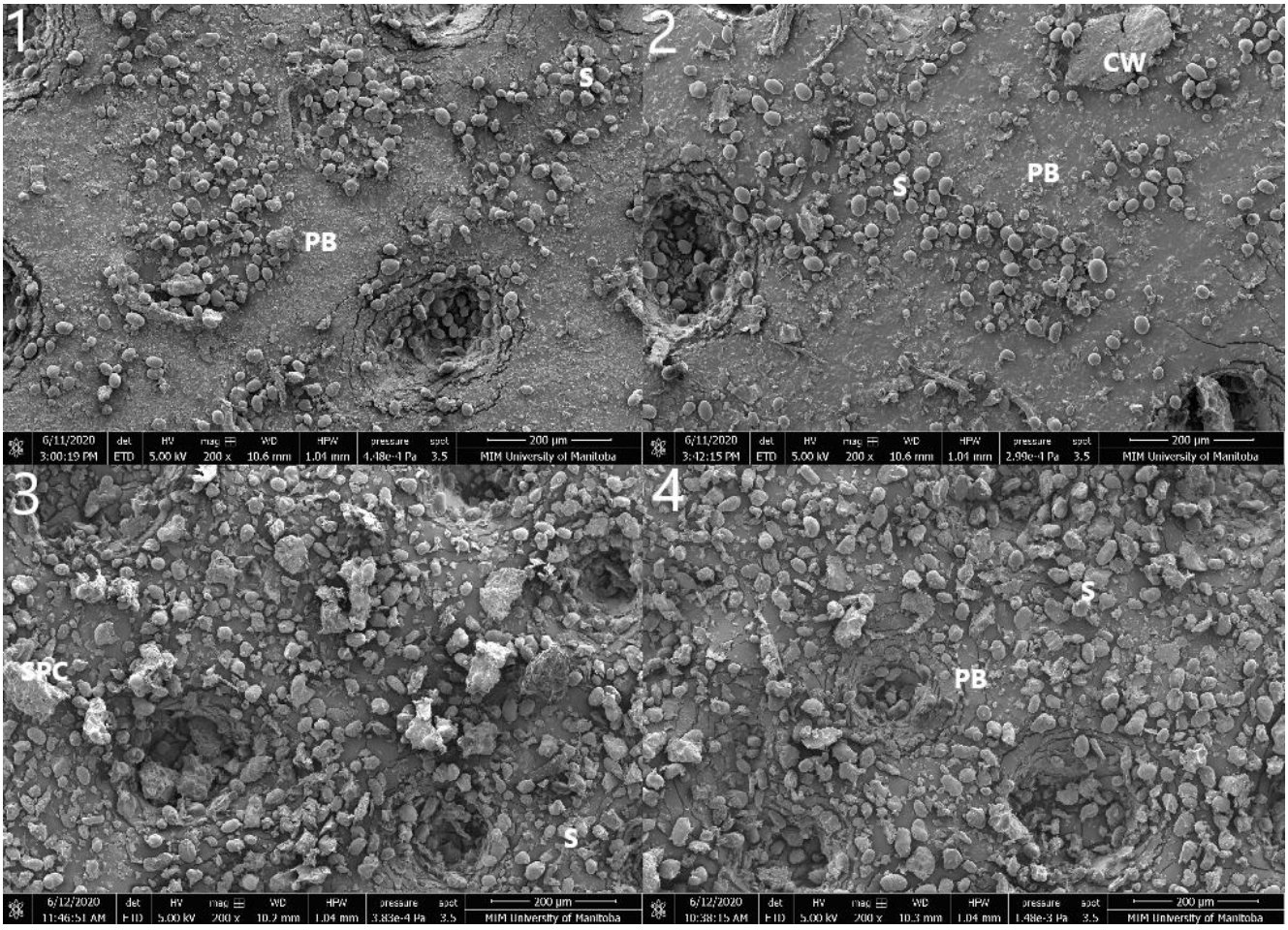

Figure 4.5. SEM images of SG stream of roller-milled (200 ×) 1) Chickpeas 2) Navy beans 3) Green lentils 4) Yellow peas. S-Starch, PB- Protein bodies, CW- Cell wall, SPC- Starch protein cluster

The micrograph of stream B1+B2+B3 is presented in supplementary Figure (SF 1 see in appendix) which showed less starch damage in comparison with the stream 1M+2M+3M (see SF 2). The micrographs of B1+B2+B3 (SF 1) flours showed higher aggregated starch granules than that of single granules. This was contrary in case of 1M+2M+3M flours (SF 2) as there were more single, unaggregated, deformed, and damaged starch granules. A similar trend was observed by Sakhare et al.(2014) for both break and reduction mung bean flours. They reported that the presence of more aggregates in break flours was due to more clearance in break roll settings. In case of reduction flours, the close grinding of the reduction rolls breaks up the highly compacted structure of the grain to protein aggregates embedding cell components, such as

starch granules. The grinding severity of milling could lead to the mechanical damage and deformation of starches. They observed that the percentage of starch damage increased as cotyledons were milled rigorously in the reduction rolls (Sakhare et al. 2014). Also, the differences in the corrugation, or that particles entering the reduction stream already display some level of particle size reduction facilitated a further degree of fineness.

4.4.3.2 SEM imaging of pulse flours across pulse-type

Figure 4.6 shows the SEM micrographs for chickpea flour streams. Chickpea flours depicted a large number of pores distributed on the granule surface compared to other pulse flours (Figure 4.6). These results are complemented by those of Zhang et al. (2019) where they observed more channels in chickpea starches. Pores of starch granules and channel structures have always been an area of scientific exploration as they assist the entry of water, enzymes, and solvents to the interior of the granules (Fannon et al. 1993; Fannon et al.1992). Fannon et al.(1992) investigated the origin of surface pores of corn starch granule and inferred that these pores could have developed due to granule formation or reactivity during granular drying, amylase action, or even as artefacts while preparing the sample for SEM.

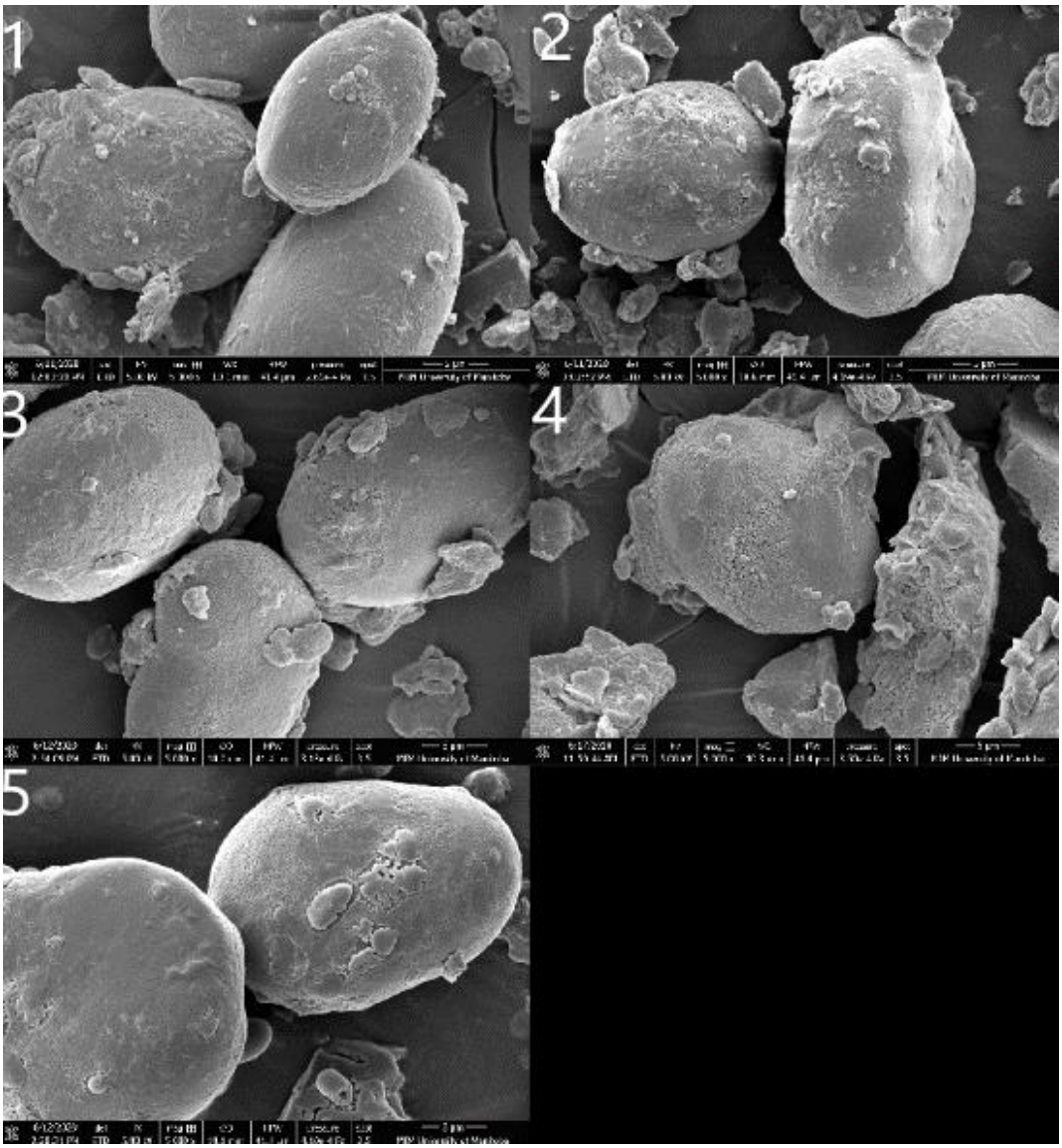

Figure 4.6. SEM images of Chickpea flours (5000×) 1) FM 2) SG 3) B1+B2+B3 4) 1M 5) 2M+3M. PB- Protein bodies, SPM- Starch-protein matrix (aggregates of starch-protein cluster)

The navy bean flours had a greater number of starch-protein matrices (aggregates of starch protein cluster) when compared to the green lentil and yellow pea flours (SF 4 and SF 5). This could be attributed to the seed hardness of pulses, a consequence of the physico-chemical bonding between the starch granules and protein (Dziki and Laskowski, 2010). The type and quantity of insoluble fibers also influences seed hardness (Wood et al. 2014). Tyler et al. (1981) reported that harder seeds have high starch-protein agglomerates with higher protein separation

efficiency in legumes. This clearly falls in line with the composition of green lentil, yellow pea, and navy bean flours.

SF 4 shows traces of seed bran in green lentil flours. Sakhare et al.(2014) reported similar results for roller-milled mung bean flours. This can be attributed to the uneven distribution of nutrients *viz.*, high protein and lipid content in embryo, starch in cotyledons and crude fibre in seed coat of green lentils (Singh and Singh , 1968). Tyler (1984) reported that milling behaviour was affected by the weak adhesion between protein bodies and starch granules due to different tissue patterns in pulses. Also, the seed morphological study and its breakage behaviour during impact or deformation gives a better understanding of the milling behaviour (Thakur et al.2019; Topin et al.2008).

4.5 Conclusion

A thorough analysis of curated data on four types of pulses and two milling methods clearly establish that both pulse-type and milling technique effect the microstructure of pulse flours. In stream-based classification, protein bodies were finely distributed in Ferkar-milled and SG stream of roller-milled flours with similar protein content. The break stream had the lowest protein content with more aggregated starch granules and less starch damage. The reduction stream had the highest protein content with more single, unaggregated, deformed, and damaged starch granules. In pulse type classification using SEM imaging, chickpea starches demonstrated a high number of pores. Navy bean flours had numerous starch-protein matrices and traces of bran were clearly visible in green lentil flours in comparison with other flours. The parameters such as uneven distribution of nutrients and seed hardness affects the milling of pulses. Therefore, it is concluded that specific pulses and milling methods are suitable for specific end products. Additional studies are recommended to optimize the milling parameters that significantly affects the flour properties to achieve desired end products.

4.6 Acknowledgements

The authors acknowledge the Pulse Cluster of the Canadian Agricultural Partnership AgriScience Program and Natural Sciences and Engineering Research Council of Canada’s Discovery Grants program for financial support. We also thank Canada Foundation for

Innovation for infrastructural support, Canadian International Grains Institute (Cigi) for their assistance in milling, and Canadian Grain Commission for whole pulse seeds nutrient values.

References

Abdullah, M. M. H., C. P. F. Marinangeli , P. J. H. Jones, and J. G. Carlberg. 2017. Canadian potential healthcare and societal cost savings from consumption of pulses: A cost-of-illness analysis. Nutrients 9(7):1–22. https://doi.org/10.3390/nu9070793.

Aguilera, J. M., and J. C. Germain. 2007. Advances in image analysis for the study of food microstructure. Understanding and Controlling the Microstructure of Complex Foods 261–287. https://doi.org/10.1533/9781845693671.2.261.

Aguilera, José Miguel. 2005. Why food micro structure? Journal of Food Engineering 67(1–2): 3–11. https://doi.org/10.1016/j.jfoodeng.2004.05.050.

Anton, A. A., K. A. Ross, O. M. Lukow, R. G. Fulcher, and S. D. Arntfield. 2008. Influence of added bean flour (Phaseolus vulgaris L.) on some physical and nutritional properties of wheat flour tortillas. Food Chemistry 109(1):33–41. https://doi.org/10.1016/j.foodchem.2007.12.005.

Assatory, A., M. Vitelli, A. R. Rajabzadeh, and R. L. Legge. 2019. Dry fractionation methods for plant protein, starch and fiber enrichment: A review. Trends in Food Science and Technology 86(February):340–351. https://doi.org/10.1016/j.tifs.2019.02.006.

Bourré, L., P. Frohlich, G. Young, Y.Borsuk, E. Sopiwnyk, A. Sarkar, … L. Malcolmson. 2019. Influence of particle size on flour and baking properties of yellow pea, navy bean, and red lentil flours. Cereal Chemistry 96(4):655–667. https://doi.org/10.1002/cche.10161.

Carlsson-Kanyama, A., and A. D. González. 2009. Potential contributions of food consumption patterns to climate change. American Journal of Clinical Nutrition 89(5):1704S-1709S. https://doi.org/10.3945/ajcn.2009.26736AA.

Cloutt, P., A. F. Walker, and D. J. Pike. 1987. Air classification of flours of three legume species: Fractionation of protein. Journal of the Science of Food and Agriculture 38(2): 177–186. https://doi.org/10.1002/jsfa.2740380209.

Diaz-contreras, L.M., R.P. Ramachandran, S. Cenkowski, and J. Paliwal. 2021. Effect of post harvest conditions on sorption isotherms of soybeans. American Society of Agricultural and Biological engineers (ASABE) 64:1027–1037.

Dziki, D., and J. Laskowski. 2010. Study to analyze the influence of sprouting of the wheat grain

on the grinding process. Journal of Food Engineering 96(4):562–567. https://doi.org/10.1016/j.jfoodeng.2009.09.002.

Fannon, J. E., Shull, M. Jeannette, and J. N. BeMiller. 1993. Interior Channels of Starch Granules. Cereal Chemistry 70(5):611–613.

Fannon, J. E., R. J. Hauber, and J. N. Bemiller. 1992. Surface pores of starch granules. Cereal Chemistry 69:284–288.

Han, J. (Jay), J. A. M. Janz, and M. Gerlat. 2010. Development of gluten-free cracker snacks using pulse flours and fractions. *Food Research International* 43(2):627–633. https://doi.org/10.1016/j.foodres.2009.07.015.

Hossain, Z., X. Wang, C. Hamel, J. Diane Knight, M.J. Morrison, and Y. Gan. 2016. Biological nitrogen fixation by pulse crops on semiarid Canadian prairies. Canadian Journal of Plant Science 97:119–131. https://doi.org/10.1139/cjps-2016-0185

Li, L., T. Z. Yuan, R. Setia, R. B. Raja, B. Zhang, and Y. Ai. 2019. Characteristics of pea, lentil and faba bean starches isolated from air-classified flours in comparison with commercial starches. Food Chemistry 276(September 2018):599–607. https://doi.org/10.1016/j.foodchem.2018.10.064.

Maskus, H., L. Bourré, S. Fraser, A. Sarkar, and L. Malcolmson. 2016. Effects of grinding method on the compositional, physical, and functional properties of whole and split yellow pea flours. Cereal Foods World 61(2):59–64. https://doi.org/10.1094/CFW-61-2-0059.

Motte, Jean-Charles, R. Tyler, A. Milani, J.Courcelles, and T.Der. 2021. Pea and lentil flour quality as affected by roller milling configuration. Legume Science 1–15. https://doi.org/10.1002/leg3.97

Osorio-Díaz, P., E. Agama-Acevedo, M. Mendoza-Vinalay, J. Tovar, and L. A. Bello-Pérez. 2008. Pasta added with chickpea flour: Chemical composition, in vitro starch digestibility and predicted glycemic index. *Ciencia y Tecnologia Alimentaria* 6(1):6–12. https://doi.org/10.1080/11358120809487621.

Pelgrom, P. J. M., R. M. Boom, and M. A. I. Schutyser. 2015. Method Development to Increase Protein Enrichment During Dry Fractionation of Starch-Rich Legumes. Food and Bioprocess Technology 8(7):1495–1502. https://doi.org/10.1007/s11947-015-1513-0.

Pelgrom, P. J. M., A. M. Vissers, R. M. Boom, and M. A. I. Schutyser. 2013. Dry fractionation for production of functional pea protein concentrates. Food Research International 53(1): 232–239. https://doi.org/10.1016/j.foodres.2013.05.004.

Pelgrom, P. J. M., J. Wang, R. M. Boom, and M. A. I. Schutyser. 2015. Pre- and post-treatment enhance the protein enrichment from milling and air classification of legumes. Journal of Food Engineering 155:53–61. https://doi.org/10.1016/j.jfoodeng.2015.01.005.

Pernollet, J. C. 1978. Protein bodies of seeds: Ultrastructure, biochemistry, biosynthesis and degradation. Phytochemistry 17:1473–1480.

Röös, E., B. Bajželj, P. Smith, M. Patel, D. Little, and T. Garnett. 2017. Protein futures for Western Europe: potential land use and climate impacts in 2050. Regional Environmental Change 17(2):367–377. https://doi.org/10.1007/s10113-016-1013-4.

Sakhare, S. D., A. A. Inamdar, S. B., D, I. Gaikwad, and V. R., G. 2014. Roller milling fractionation of green gram (Vigna radiata): optimization of milling conditions and chemical characterization of millstreams. Journal of Food Science and Technology 51(12): 3854–3861. https://doi.org/10.1007/s13197-012-0903-9.

Scanlon, M.G., S. Thakur, R.T. Tyler, A. Milani, T. Der, and J. Paliwal. 2018. The critical role of milling in pulse ingredient functionality. Cereal Foods World 63:201–206. https://doi.org/10.1094/CFW-63-5-0201

Schutyser, M. A. I., P. J. M. Pelgrom, A. J. van der Goot, and R. M. Boom. 2015. Dry fractionation for sustainable production of functional legume protein concentrates. Trends in Food Science and Technology 45(2):327–335. https://doi.org/10.1016/j.tifs.2015.04.013.

Schutyser, M. A. I., and A. J. van der Goot. 2011. The potential of dry fractionation processes for sustainable plant protein production. Trends in Food Science and Technology 22(4):154–164. https://doi.org/10.1016/j.tifs.2010.11.006

Singh S and S. K. Singh HD. 1968. Distribution of nutrients in the anatomical part of common Indian pulses. Cereal Chemistry 45:13–18.

Thakur, S., M. G. Scanlon, R. T.Tyler, A. Milani, and J. Paliwal. 2019. Pulse Flour Characteristics from a Wheat Flour Miller's Perspective: A Comprehensive Review. Comprehensive Reviews in Food Science and Food Safety 18(3):775–797. https://doi.org/10.1111/1541-4337.12413.

Topin, V., F. Radjaï, J. Y. Delenne, A. Sadoudi, and F. Mabille. 2008. Wheat endosperm as a cohesive granular material. Journal of Cereal Science 47(2):347–356. https://doi.org/10.1016/j.jcs.2007.05.005.

Tyler, R. T., C. G. Youngs, and F. W. Sosulski. 1981. Air classification of legumes. I. Separation efficiency, yield and composition of the starch and protein fractions. Cereal Chemistry 58(May):144–148. Retrieved from https://www.aaccnet.org/publications/cc/backissues/1981/Documents/chem58_144.pdf

Tyler, T. 1984. Pin Mill , Air Classify. Journal of Food Science 49:925–930.

Williams, P., D. Sobering, and J. Antoniszyn. 1998. Protein testing methods at the Canadian Grain Commission. Wheat Protein, Production and Marketing, Proceedings of the Wheat Protein Symposium 37–47.

Wood, J. A., E. J. Knights, G. M. Campbell, and M. Choct. 2014. Differences between easy- and difficult-to-mill chickpea (Cicer arietinum L.) genotypes. Part I: Broad chemical composition. Journal of the Science of Food and Agriculture 94(7):1437–1445. https://doi.org/10.1002/jsfa.6437.

Young, V. R., and P. L. Pellett. 1994. Plant proteins in relation to human protein and amino acid nutrition. American Journal of Clinical Nutrition, 59(5 SUPPL.). https://doi.org/10.1093/ajcn/59.5.1203S.

Zhang, Z., X. Tian, P. Wang, H. Jiang, and W. Li. 2019. Compositional, morphological, and physicochemical properties of starches from red adzuki bean, chickpea, faba bean, and baiyue bean grown in China. Food Science and Nutrition 7(8):2485–2494. https://doi.org/10.1002/fsn3.865.

CHAPTER 5. Thesis summary and overall conclusion

The research explores the potential use of non-destructive methods for characterizing pulse flours. From HSI results, it can be established that pulse flour-type can be classified using Vis-NIR range on the basis of color attributes with green and yellow bands playing a significant role in classification. The milling method can be classified using SWIR range on the basis of chemical composition with the wavelengths attributed to protein content playing a major role. For classification purposes, reliable results were acquired from the supervised classification using PLS-DA. It can be concluded that both wavelength ranges contributed towards the classification goals but the classification accuracy in terms of milling method can be enhanced by enlarging the dataset.

SEM images revealed that different milling methods affect the microstructural properties of pulse flours distinctly. There is an indirect relation between particle size distribution and protein content. Protein bodies are finely distributed in Ferkar mill and SG stream of roller-milled flours with similar protein content. The micrographs of B1+B2+B3 (possessing lowest protein content) and 1M+2M+3M (possessing highest protein content) streams of roller milled flours showed that the former was more aggregated with less starch damage whereas the latter had unaggregated starch granules with more starch damage. The presence of visible pores was prominent in chickpea starches; navy bean flours had more starch protein cluster counts and traces of bran particles were clearly visible in green lentil flours. Seed hardness affects pulse milling with variations in nutrient composition. Overall, it can be concluded that non-destructive techniques can be used for classification of pulse flours.

CHAPTER 6. Recommendations for future research

Challenges in the current research:

- The results of classification of pulse flours based on streams in the SWIR range were not encouraging. The flours were classified for break and reduction stream because of the variation in the protein content. Owing to the similar chemical composition for the rest of the flour streams, the groupings were not encouraging.
- The distribution of cell components in the pulse seeds prior to milling plays an important role in the separation of cell components in pulse flours to obtain protein/starch enriched fractions.

Recommendations:

- FTIR studies need to be carried out to characterize the pulse flours in the mid infrared range. Classification models can then be developed based on pulse-flour type, milling method, and stream-based classification for pulse flours. Prediction models for protein content can be developed as well.
- Whole pulse seeds can be studied using SEM to understand the milling characteristics and distribution of cell components.

APPENDIX 1

Table 7.1 % Protein content of flour samples with replicates FM- Ferkar mill, SG- straight grade, B1+B2+B3- break flour, 1M+2M+3M; 1M; 2M+3M- Reduction flours, CP-Chickpea, NB-navy bean, GL -green lentil, YP- yellow pea

SL. NO	FM				SG				B1+B2+B3			
	CP	NB	YP	GL	CP	NB	YP	GL	CP	NB	YP	GL
1	17.61	23.03	22.52	22.13	18.27	23.62	22.54	23.78	16.41	19.41	19.69	22.35
2	18.04	23.20	22.66	22.46	18.22	23.62	22.63	23.66	16.08	18.72	19.58	22.34
3	17.86	23.30	22.57	22.65	17.34	23.38	22.25	23.64	16.43	19.47	19.79	21.43
4	17.63	23.15	22.47	22.64	17.00	23.52	22.51	23.62	16.47	19.73	19.77	22.27
5	18.28	23.72	22.24	22.68	19.50	23.64	22.67	23.39	16.58	19.91	19.72	22.45
6	18.02	23.43	22.10	22.55	18.12	23.34	22.56	23.58	16.54	19.32	19.83	22.46
7	17.99	23.34	22.12	22.67	17.73	23.46	22.72	24.01	16.60	19.15	19.25	22.42
8	18.33	23.20	22.18	22.41	18.21	23.36	22.67	23.53	16.62	19.50	19.45	22.43

SL. NO.	1M+2M+3M		1M		2M+3M	
	YP	GL	CP	NB	CP	NB
1	22.51	23.82	18.08	23.33	19.28	26.69
2	22.35	23.97	17.33	23.07	19.18	26.59
3	23.03	23.78	18.10	23.44	20.16	26.76
4	23.20	23.72	18.14	23.30	19.12	26.33
5	23.26	23.86	18.46	23.42	19.89	27.23
6	23.31	23.74	18.34	23.56	19.94	26.68
7	23.23	23.62	18.03	23.57	20.37	26.34
8	23.32	23.74	18.10	23.55	19.53	26.64

SUPPLEMENTARY FIGURES

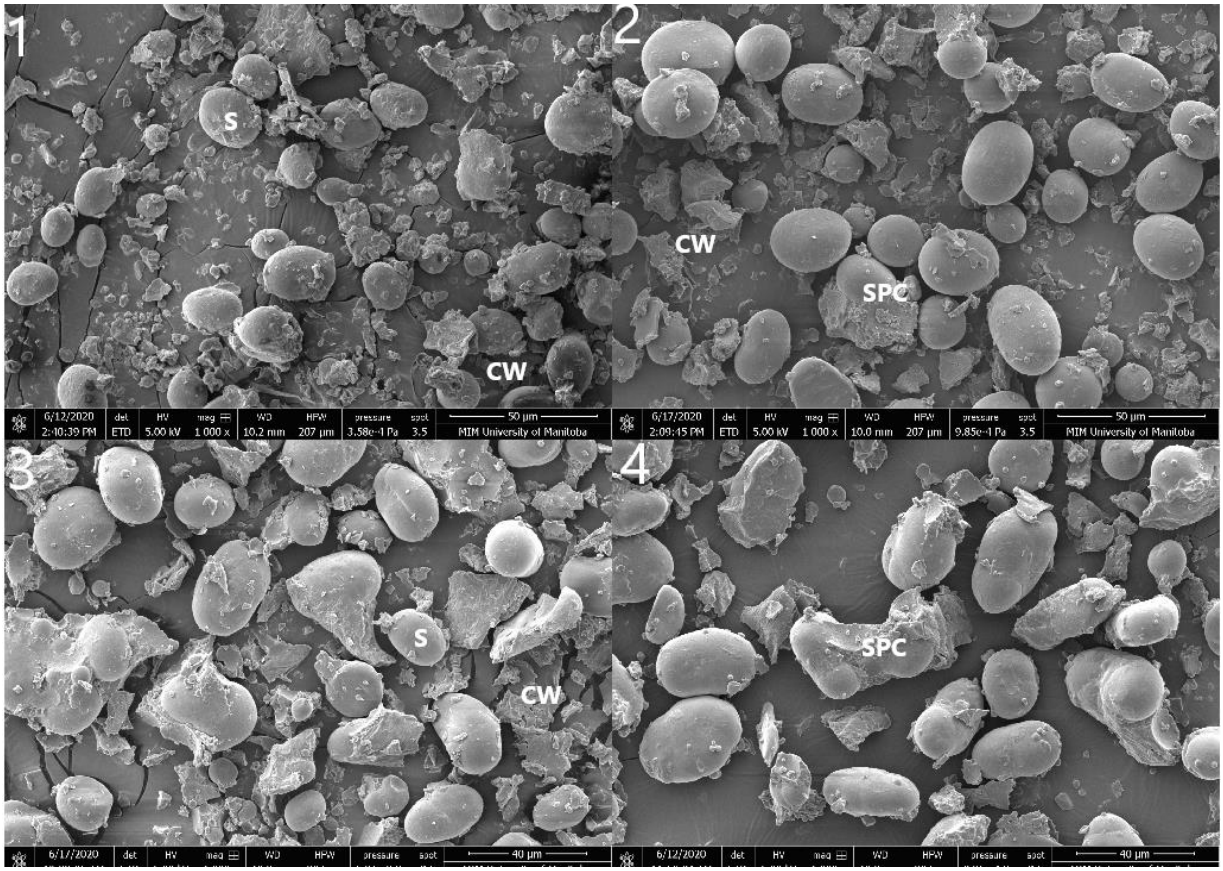

SF 1. SEM images of B1+B2+B3 stream of roller mill (1000×) 1) Chickpeas 2) Navy beans 3) Green lentils 4) Yellow peas. S-Starch, PB- Protein bodies, CW- Cell wall, SPC- Starch protein cluster

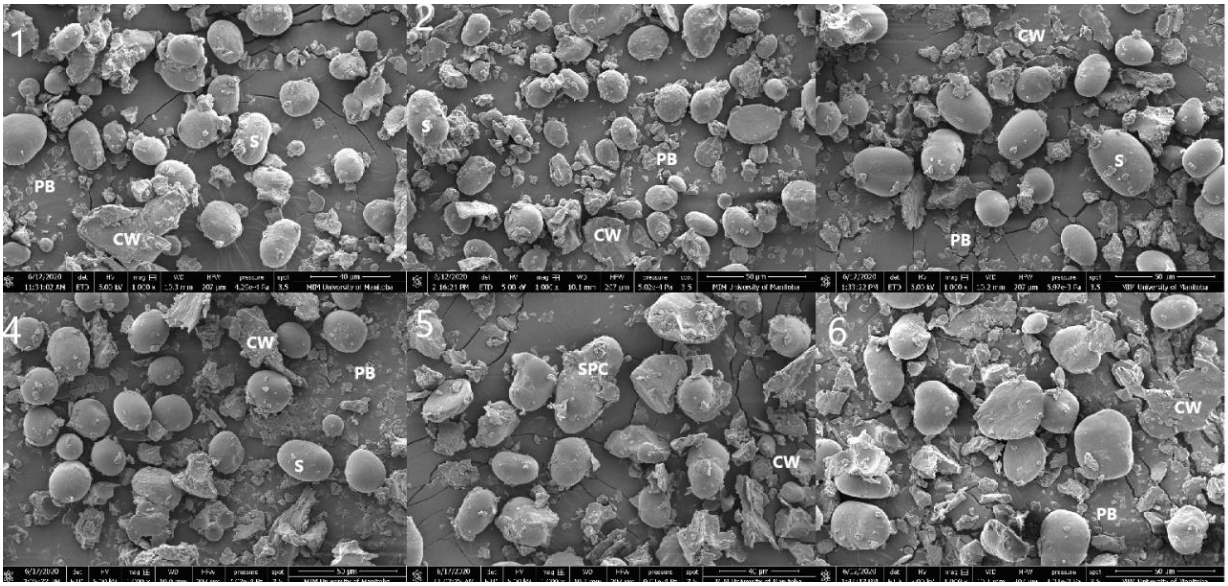

SF 2. SEM images of 1M+2M+3M stream of roller mill (1000×) 1) Chickpeas (1M) 2) Chickpeas (2M+3M) 3) Navy beans (1M) 4) Navy beans (2M+3M) 5) Green lentils (1M+2M+3M) 6) Yellow peas (1M+2M+3M). S-Starch, PB- Protein bodies, CW- Cell wall, SPC- Starch protein cluster

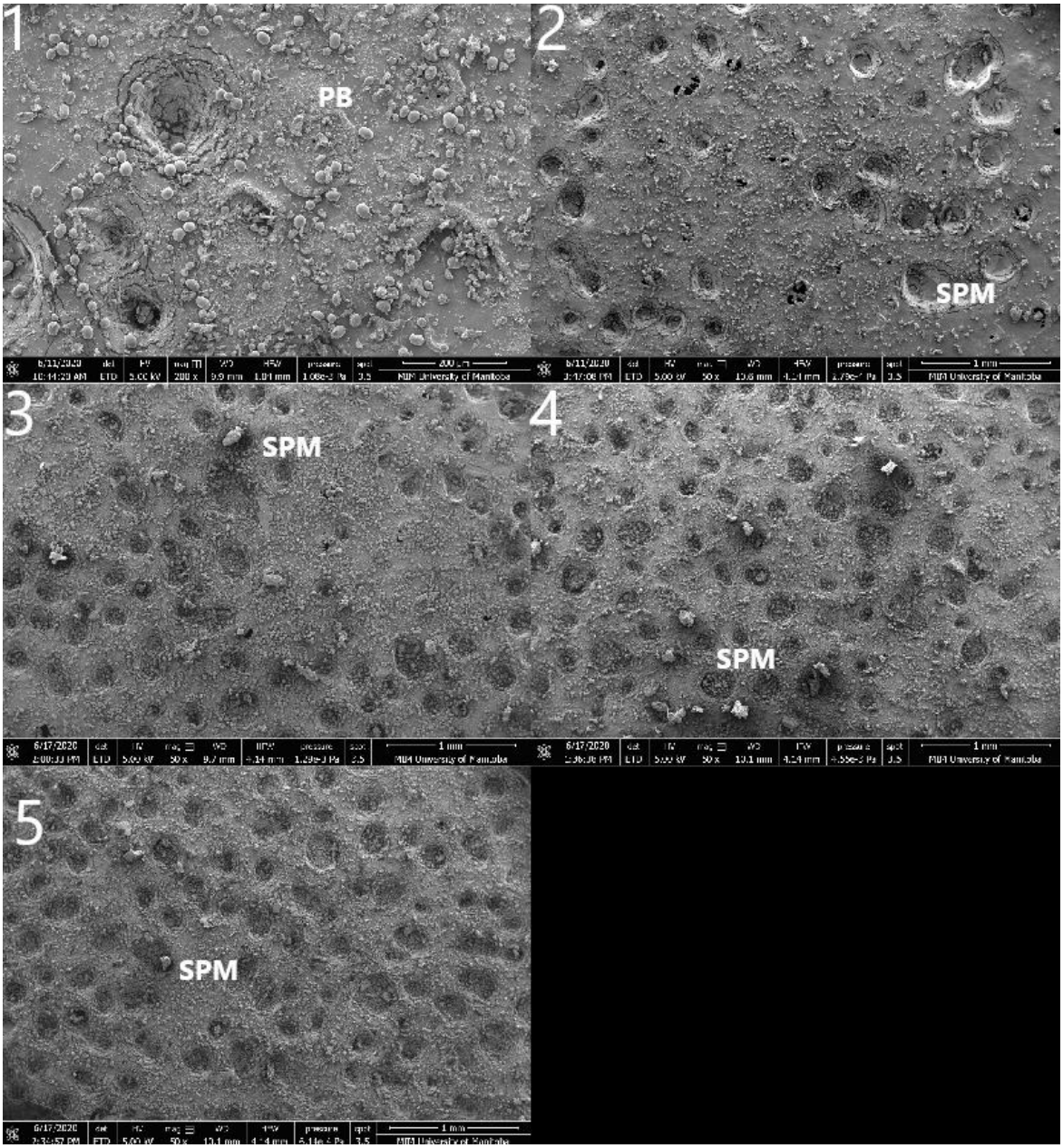

SF 3. SEM images of Navy beans flours 1) FM (200×) 2) SG (50x) 3) B1+B2+B3 (50x) 4) 1M (50x) 5) 2M+3M (50x). PB- Protein bodies, SPM- Starch protein matrix (aggregates of starch protein cluster)

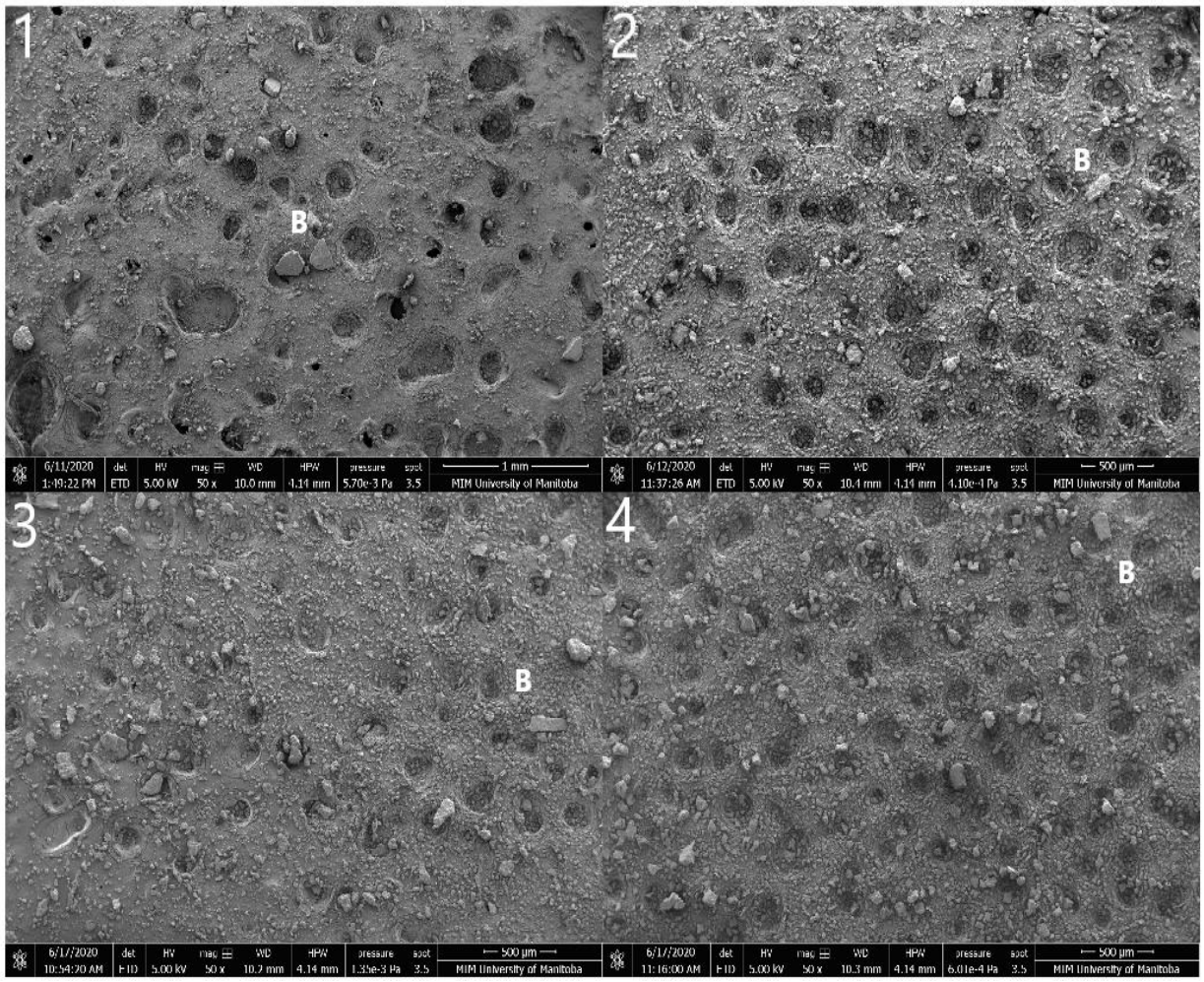

SF 4. SEM images of green lentils flours (50×) 1) FM 2) SG 3) B1+B2+B3 4) 1M+2M+3M. SPM- Starch protein matrix (aggregates of starch protein cluster)

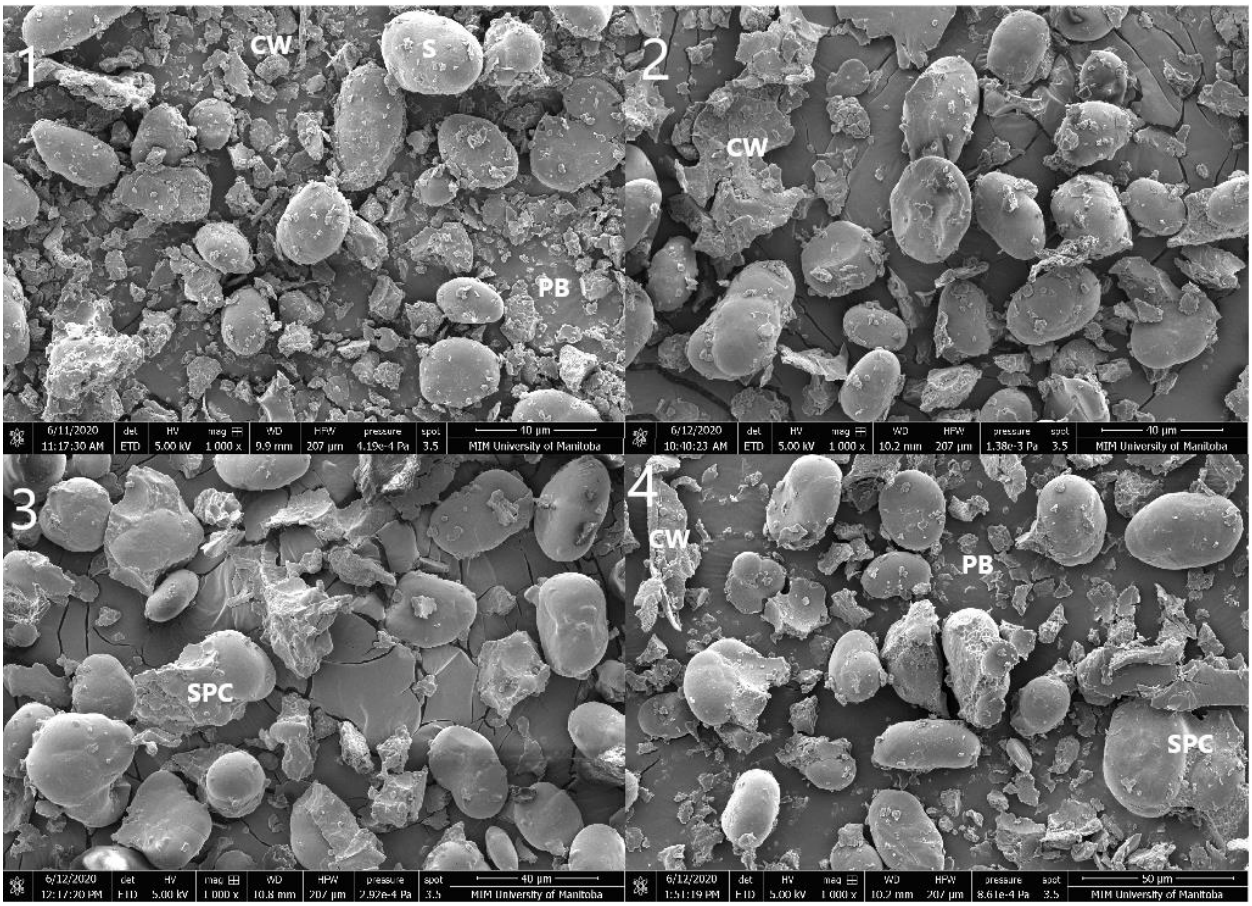

SF 5. SEM images of yellow peas flours (200 ×) 1) FM 2) SG 3) B1+B2+B3 4) 1M+2M+3M. PB- Protein bodies, CW- Cell wall, SPC- Starch protein cluster